

# Effects from New Colored States and the Higgs Portal on Gluon Fusion and Higgs Decays

Kunal Kumar<sup>\*</sup> and Roberto Vega-Morales<sup>†</sup>

*Northwestern University, 2145 Sheridan Road, Evanston, IL 60208, USA*

Felix Yu<sup>‡</sup>

*Theoretical Physics Department, Fermilab, Batavia, IL 60510, USA*

We study effects from new colored states and the Higgs portal on gluon fusion production. We isolate possible loop contributions from new colored scalars, fermions, and vectors, incorporating effects from Higgs portal-induced scalar mixing, thus leading to dramatic effects on gluon fusion and branching fractions. Higgs identification must generally allow for these effects, and using our results, possible tensions from fits to the Standard Model expectation can be relieved by inclusion of New Physics effects.

---

<sup>\*</sup> kkumar@u.northwestern.edu

<sup>†</sup> robertovegamorales2010@u.northwestern.edu

<sup>‡</sup> felixyu@fnal.gov

## I. INTRODUCTION

The ATLAS [1] and CMS [2] experiments at the Large Hadron Collider (LHC) have recently presented results that indicate the observation (also supported by evidence coming from the 1.96 TeV run of the Tevatron [3]) of a new resonance. When interpreted as a Standard Model (SM) Higgs, the combined channels are consistent with the SM expectation at  $1\sigma$ , yet individual channels show deviations from the SM expectation in the  $1\text{--}2\sigma$  range. The discovery of the Higgs boson would certainly be one of the most exciting developments in particle physics to date and it is tempting to assume this new resonance is indeed the Higgs, but establishing the true nature of this excess as the SM Higgs must still proceed with due diligence.

The two main theoretical inputs in performing such a Higgs identification are the Standard Model branching fractions for each of the decay channels used in the combination and the overall Higgs production cross section. We highlight that Higgs production from gluon fusion, the dominant production mode at hadron colliders, occurs via loops of SM quarks and is hence uniquely sensitive to New Physics (NP) effects arising from new colored states [4–26] or more general Higgs portal [27–39] and scalar mixing effects [40–44]. The  $\gamma\gamma$  branching fraction, which arises at loop-level in the Standard Model [45], is similarly sensitive to NP effects [46–50]. For example, in the well-studied four generation Standard Model (SM4), gluon fusion rates are enhanced while the branching ratio to diphotons is suppressed [46, 51–61].

Moreover, the landmark discovery of a Standard Model Higgs crucially relies on affirming the hypothesis of the Higgs mechanism for spontaneous breaking of  $SU(2)_L \times U(1)_Y$  gauge symmetry, which predicts the existence of the Higgs boson. This fundamental test can only come after directly measuring the Higgs couplings to the  $SU(2)$  gauge bosons. The fact that the Higgs is responsible for chiral symmetry breaking in the Standard Model and hence gives fermion masses is only a byproduct of the Higgs mechanism, and thus, in particular, the gluon fusion Higgs production mode does not directly probe the Higgs mechanism. This implies that NP could still be hiding in the gluon fusion process without effecting EWSB.

This crucial point, which has also been emphasized in several recent papers [19, 20, 32, 35, 38], means that the LHC Higgs searches can be skewed by the presence of new colored particles which positively or negatively contribute to gluon fusion. Moreover, the excess in the data should be interpreted not only in the context of a SM Higgs, but also in the more exciting scenario of a possible new scalar state which arises from a Higgs portal-induced mixing between the SM Higgs and a new scalar. We demonstrate that extended color sectors involving new colored particles will

generally give rise to both effects. In particular, if the new colored particles do not get their mass from the vacuum expectation value (vev) of the Higgs boson, then a generic Higgs portal term can give rise to Higgs mixing. We can see that direct Higgs coupling and Higgs portal-induced scalar mixing are two important categories of NP contributions that can have marked effects on Higgs collider signals, and thus we consider them simultaneously.

Motivated by the possibility of probing new colored states via gluon fusion, we adopt a building block approach for an arbitrary NP model. Namely, we isolate and calculate the gluon fusion amplitude for new colored scalars, fermions, and vectors. In the case of the colored vector, we present the calculation in the context of the renormalizable coloron model (ReCoM) [62–64] such that the concomitant effects from maintaining UV consistency can be readily included. We also allow for Higgs mixing, where the SM Higgs is mixed with a new scalar. In addition, for a mild and well-motivated set of assumptions, we give generic expressions for branching ratios of the scalar mass eigenstates into the most sensitive SM Higgs decay modes.

Since our work has some overlap with many studies in the literature, we survey several representative papers and elaborate on the differences. A few recent papers have focused on our first category of NP effects for  $gg \rightarrow h$  in which the NP states couple directly to the SM Higgs. In particular, the authors of [32] focused solely on the situation where new particle masses arise from the Higgs vev, which simultaneously sharpens their discussion of resulting gluon fusion and diphoton decay phenomenology and limits the breadth of their conclusions. Separately, the authors of [20] focused on Higgs portal phenomenology with new colored scalars, while the work in [33, 35] also included new scalars transforming under the full SM gauge symmetry. A similar study, emphasizing the constraints from electroweak precision fits, was performed in [18, 19]. We go beyond these direct coupling studies by also including the effects of a colored vector.

There have also been a number of recent studies [65, 66] where fits are performed in order to determine how consistent the data is with a SM Higgs hypothesis. These studies find that generally the excess is largely consistent with a SM Higgs with a tantalizing, but small enhancement in the  $\gamma\gamma$  channel. However, these fits still have large uncertainties, and the next data set can change the picture drastically. Also, the Higgs couplings to bosons rely heavily on the vector boson fusion channel, which has large fluctuations between 7 and 8 TeV. These uncertainties leave room for modifications to the coupling of the SM Higgs to gluons which can be either enhanced or suppressed given the sign of the Higgs portal term. We will examine this in detail below.

Regarding our second category of NP effects, when the SM Higgs mixes with a new scalar via a Higgs portal term, a majority of the literature has focused on the case where the New Physics

sector is completely invisible to the SM [27–30, 34, 36, 39], providing a possible connection to the dark matter. In this situation, as we will see in Sec. II, only a simple mixing angle is needed to parametrize the effects on Higgs phenomenology, if no new decays are kinematically allowed. Our work considers the more complicated scenario where the new scalar couples to new colored particles, similar to [35], as mentioned above.

In addition to these renormalizable scenarios of NP effects on loop-induced SM Higgs phenomenology, a few papers have followed an effective field theory approach by constructing and constraining the size of dimension-six operators. In [7], the authors focused on the coefficients and constraints of operators for  $h \rightarrow \gamma\gamma$ ,  $\gamma Z$ , and  $gg$ , while [12] extended the discussion to include  $h \rightarrow f\bar{f}$  as well. Importantly, both of these studies assume any New Physics contributions are heavy enough to be integrated out, thus there are no new particles in the low energy spectrum.

In contrast to the previous literature, therefore, we discuss the general case using renormalizable interactions when both categories of NP effects are present. We isolate contributions with new colored scalars, new colored fermions, including Standard Model quark mixing, and new colored vectors, and we allow such effects to be modified by Higgs mixing.

The paper is organized as follows. In Sec. II, we discuss general aspects of the Higgs portal relevant for our analysis of Standard Model Higgs production from gluon fusion. In Sec. III, we briefly review the leading order  $gg \rightarrow h$  calculation for the Standard Model as well as the trivial extension of adding a fourth generation. In Sec. IV, we discuss gluon fusion in the presence of a new colored scalar. In Sec. V, we present the analogous calculation for a general new colored fermion. Lastly, in Sec. VI, we discuss the interesting case of a new colored vector and its effects on gluon fusion in the context of a UV-complete, renormalizable model. Details of this calculation are presented in Appendix A. We summarize and conclude in Sec. VII.

## II. THE HIGGS PORTAL AND HIGGS MIXING

In this section, we review the Higgs portal as a general framework for studying the connection between arbitrary New Physics models and Higgs physics, with a special emphasis on the resulting effect on gluon fusion.

In the SM, the Higgs field is responsible for breaking  $SU(2)_L \times U(1)_Y$  gauge symmetry, resulting in masses for the  $W^\pm$  and  $Z$  bosons as well as the chiral SM fermions. By virtue of being the only scalar field present in the SM, the Higgs also generates  $H^\dagger H$ , which is the lowest mass dimension operator possible in the SM that is both gauge and Lorentz invariant. Hence, arbitrary

NP operators can then be tacked on to  $H^\dagger H$  to give

$$\mathcal{L}_{hp} \supset \lambda_{hp} \mathcal{O}_{NP} H^\dagger H . \quad (1)$$

Although  $\mathcal{O}_{NP}$  can be an arbitrarily high dimension operator, with an appropriate power suppression from a high scale  $\Lambda_{NP}$ , a generic Higgs portal term is only typically unsuppressed when  $\mathcal{O}_{NP}$  itself is dimension two and gauge and Lorentz invariant: hence, we take  $\mathcal{O}_{NP} \sim \Phi^\dagger \Phi$ . One exception is the case when a new scalar field is a pure SM and NP gauge singlet, but since we are focused on NP effects on gluon fusion, we will not discuss the gauge singlet case further.

One class of NP effects on gluon fusion arises from new colored states that directly enter the  $gg \rightarrow h$  loop diagram. The direct coupling of colored states to the Higgs via Eq. (1) implies the mass of the new state is shifted after electroweak symmetry breaking (EWSB), and as this direct coupling is turned off, the NP effect vanishes. This class of effects is typified by models with new colored scalars, but a new fermion with Yukawa-like couplings to the SM Higgs boson also follows this scheme, albeit not via the Higgs portal. Although the case where the mass of the NP state arises primarily from the Higgs vev was discussed in [32], in our more general framework the NP mass scale and the new couplings to the SM Higgs are independent.

Since new particle masses do not have to arise from the SM Higgs vev, a second broad class of NP effects on gluon fusion emerges. Namely, if a new scalar field obtains a vev to spontaneously break a new gauge symmetry and if a Higgs portal term is present, this new scalar field will mix with the SM Higgs. In this class, NP effects coming from new colored states can infiltrate gluon fusion through the mixing induced from the Higgs portal even if these states do not directly couple to the SM Higgs. These effects will also exhibit the familiar non-decoupling features in SM  $gg \rightarrow h$  loop calculations by chiral fermions or  $h \rightarrow \gamma\gamma$  loop calculations by  $W$  bosons if the analogous NP states are present [45, 67, 68]: however, this non-decoupling feature only applies to the new scalar field component of the scalar mass eigenstates.

As mentioned in the introduction, we allow for both direct and Higgs mixing mediated categories of NP effects to be present simultaneously. These effects arise in many extended color sector models, and we consider isolated new colored scalars, fermions, and vectors in turn. For colored scalars, we couple them to the Higgs via the Higgs portal in Eq. (1), and hence they will exhibit an example of the direct category of NP effects with  $\lambda_{hp}$  as the direct coupling. For colored fermions, we consider two subcategories distinguished by the possibility of SM fermion mixing. If new fermions are introduced that mix with SM fermions, the usual SM calculation is modified to accommodate fermion mass eigenstates that do not typically couple with the SM Higgs with the usual Yukawa

strength. Without such fermion mixing, the SM calculation is unchanged and the new contribution arises from direct Yukawa couplings to the Higgs, the new scalar, or both. The decoupling behavior of new colored fermions are parametrized by fermion mixing angles and the possible scalar mixing angle.

Perhaps the most interesting case is that of a massive colored vector boson. Here, in order to have a theory which is tree level unitary [69], it is natural to consider an extended color symmetry which is then spontaneously broken to  $SU(3)_c$  gauge symmetry. Then the massive vectors corresponding to the broken generators form representations of the unbroken color symmetry. We are thus left with a renormalizable, unitary, spontaneously broken gauge theory [70].

We remark that another class of New Physics effects via the Higgs portal operator is possible. Broadly speaking, at the renormalizable level, where  $\mathcal{O}_{NP} \sim \Phi^\dagger \Phi$  in Eq. (1), one class of Higgs portal effects is characterized by new colored scalars which do not obtain vevs. The second class is driven by new uncolored scalars that do obtain vevs from their scalar potential. Another possibility is colored scalars that do obtain vevs, but such color-breaking vacua are not viable phenomenologically. The last possibility consists of new uncolored scalars that do not obtain vevs from their scalar potential. Such a scalar does not enter the  $gg \rightarrow h$  loop, but if  $\lambda_{hp}$  is large and positive, the resulting Higgs portal-induced shift in mass squared,  $-\lambda_{hp}v_h^2$  ( $v_h$  is the Higgs vev) could drive the new scalar to acquire a vev. Hence, this last category of portal symmetry breaking models is unique because the Higgs portal coupling is a necessary ingredient for driving the new scalar to obtain a nonzero vev. Obviously, the roles of the new scalar and the Higgs scalar can be reversed, whereby the Higgs portal term allows a new scalar vev to drive the Higgs field to obtain a negative mass squared and hence trigger EWSB. We reserve a study of “Portal Symmetry Breaking” phenomenology for future work. Also, in the discussion above, we have delineated cases according to specific constraints on the Lagrangian parameters. A precise determination of these bounds would require an analysis of renormalization group evolution, which is beyond the scope of this work.

### A. New Physics Scalar – Standard Model Higgs Mixing

We briefly discuss the second class of NP effects from the Higgs portal described above, *i.e.* a new scalar and the SM Higgs both obtain vevs in Eq. (1) and mix. For simplicity, we only consider one new scalar, but our discussion is readily generalized to multiple scalars. We also assume  $\Phi$  transforms as a singlet under  $SU(2)_L \times U(1)_Y$ , but that it is charged under a new local or global

symmetry in order to prevent "tadpole" terms. We let  $\mathcal{O}_{NP} \sim \Phi^\dagger \Phi$  for a new scalar field  $\Phi$ , giving

$$\mathcal{L} \supset \lambda_{hp} H^\dagger H \Phi^\dagger \Phi \sim \lambda_{hp} v_h v_\phi h \phi , \quad (2)$$

where we have suppressed representation indices and expanded the fields  $H \sim \frac{1}{\sqrt{2}}(h + v_h)$  and  $\Phi \sim \frac{1}{\sqrt{2}}(\phi + v_\phi)$ . We assume the scalar potentials  $V(\Phi)$  and  $V(H)$  are also present and Eq. (2) is the only Lagrangian term involving both  $\Phi$  and  $H$  fields. The usual stability, triviality, and renormalizability constraints on the full scalar potential  $V(H) + V(\Phi) - \lambda_{hp}|H|^2|\Phi|^2$  are assumed to be satisfied and will be imposed when we consider explicit models in Secs. V and VI. Here, since  $\Phi$  obtains a vev, Eq. (2) leads to mixing via the mass matrix

$$m_{\text{scalar}}^2 = \begin{pmatrix} m_h^2 & -\lambda_{hp} v_h v_\phi \\ -\lambda_{hp} v_h v_\phi & m_\phi^2 \end{pmatrix} , \quad (3)$$

where  $v_h$  and  $v_\phi$  are calculated from minimizing the full potential  $V(H) + V(\Phi) - \lambda_{hp}|H|^2|\Phi|^2$  and hence determine  $m_h$  and  $m_\phi$ . The functional dependence of  $m_h$  and  $m_\phi$  on their respective potential parameters can be fixed by solving the potentials  $V(H)$  and  $V(\Phi)$  separately, and in the limit that  $\lambda_{hp} \rightarrow 0$ , the exact vevs  $v_h$  and  $v_\phi$  recover their original, unperturbed values. This observation has important ramifications when calculating the exact Goldstone–Goldstone–scalar couplings needed for vector loop amplitudes in Feynman gauge, which are discussed in Subsec. A 3.

We can readily diagonalize the symmetric mass matrix Eq. (3) to obtain the mass eigenstates

$$\begin{aligned} s_1 &= h \cos \theta - \phi \sin \theta , \\ s_2 &= h \sin \theta + \phi \cos \theta , \end{aligned} \quad (4)$$

with a Jacobi rotation mixing angle  $\theta$  defined by

$$\tan 2\theta = \frac{-2\lambda_{hp} v_h v_\phi}{m_\phi^2 - m_h^2} . \quad (5)$$

We will also need the inverse operations,

$$\begin{aligned} h &= s_1 \cos \theta + s_2 \sin \theta , \\ \phi &= -s_1 \sin \theta + s_2 \cos \theta . \end{aligned} \quad (6)$$

The eigenvalues of Eq. (3) are

$$m_{s_1}^2 = \frac{1}{2} (m_h^2 + m_\phi^2) - \frac{1}{2} \sqrt{\left(-m_h^2 + m_\phi^2\right)^2 + 4\lambda_{hp}^2 v_h^2 v_\phi^2} , \quad (7)$$

and

$$m_{s_2}^2 = \frac{1}{2} (m_h^2 + m_\phi^2) + \frac{1}{2} \sqrt{\left(-m_h^2 + m_\phi^2\right)^2 + 4\lambda_{hp}^2 v_h^2 v_\phi^2} , \quad (8)$$

where we have taken  $m_{s_1} < m_{s_2}$  without loss of generality. As mentioned before and demonstrated in [27, 30, 35], the mixing of the scalar states from the Higgs portal can significantly affect scalar production via gluon fusion. Moreover, the mixing is driven purely by the strength of  $\lambda_{hp}$ , which must be real but whose sign is not fixed.

### B. New Physics Effects on Production of $s_{1,2}$

We can now readily disentangle the two categories of New Physics effects on gluon fusion. Now, because of  $h$ - $\phi$  mixing via the Higgs portal in Eq. (2), we must calculate cross sections for  $gg \rightarrow s_1$  and  $gg \rightarrow s_2$  production instead of the gauge eigenstates  $h$  and  $\phi$ . Since both  $h$  and  $\phi$  can couple to new colored particles, contributions to  $gg \rightarrow s_{1,2}$  can manifest themselves through both the  $h$  and  $\phi$  components of  $s_{1,2}$ , leading to suppression or enhancement of the production rate relative to the SM. This also implies that partial decay widths are affected, whereas in hidden sector models, such widths are unaltered apart from a universal  $\cos^2 \theta$  suppression coming from Higgs mixing.

From the discussion above, we can decompose the production amplitude of  $s_1$  via gluon fusion in terms of the gauge eigenstate  $h$  and  $\phi$  production amplitudes as,

$$\begin{aligned}\mathcal{M}(gg \rightarrow s_1) &= c_\theta [\mathcal{M}(gg \rightarrow h)]|_{m_h=m_{s_1}} - s_\theta [\mathcal{M}(gg \rightarrow \phi)]|_{m_\phi=m_{s_1}} \\ \mathcal{M}(gg \rightarrow s_2) &= s_\theta [\mathcal{M}(gg \rightarrow h)]|_{m_h=m_{s_2}} + c_\theta [\mathcal{M}(gg \rightarrow \phi)]|_{m_\phi=m_{s_2}},\end{aligned}\tag{9}$$

where  $c_\theta \equiv \cos \theta$ ,  $s_\theta \equiv \sin \theta$  are defined by Eq. (5). In the discussion below, we presume the matrix elements are evaluated at the appropriate scalar mass and will drop the notation above. Hence, given the linear combination dictated by Eq. (9), we are now free to isolate the contributions to  $gg \rightarrow h$  and  $gg \rightarrow \phi$ .

We are particularly interested in identifying, at the amplitude level, the mechanisms responsible for modifying gluon fusion and whether and how they can decouple. A completely general expression for all possible NP effects along these lines is cumbersome, so instead we write

$$\begin{aligned}\mathcal{M}(gg \rightarrow s_1) &= c_\theta \left[ \mathcal{M}(gg \xrightarrow{\text{scalars}} h) + \mathcal{M}(gg \xrightarrow{\text{fermions}} h) + \mathcal{M}(gg \xrightarrow{\text{vectors}} h) \right] \\ &- s_\theta \left[ \mathcal{M}(gg \xrightarrow{\text{scalars}} \phi) + \mathcal{M}(gg \xrightarrow{\text{fermions}} \phi) + \mathcal{M}(gg \xrightarrow{\text{vectors}} \phi) \right],\end{aligned}\tag{10}$$

and treat each category of loop particles separately.<sup>1</sup> Each of these categories can be further subdivided into particles that couple solely to  $h$ , solely to  $\phi$ , or simultaneously to both. In the

---

<sup>1</sup> For the vector loop calculation, we implicitly assume a unitary gauge calculation where only vectors appear in the loop. If working in Feynman gauge, the associated Goldstone and ghosts would also be part of the vector category.



scalar case, for example, we can write

$$\begin{aligned} \mathcal{M}(gg \xrightarrow[\text{scalars}]{} s_1) &= c_\theta \left[ \sum_i \mathcal{M}(gg \xrightarrow{\eta_i} h) + \sum_j \mathcal{M}(gg \xrightarrow{\eta_j} h) \right] \\ &- s_\theta \left[ \sum_j \mathcal{M}(gg \xrightarrow{\eta_j} \phi) + \sum_k \mathcal{M}(gg \xrightarrow{\eta_k} \phi) \right], \end{aligned} \quad (11)$$

where the scalars  $\eta_i$ ,  $\eta_j$ ,  $\eta_k$  couple only to  $h$ , both to  $h$  and  $\phi$ , and only to  $\phi$ , respectively. We can now make definitive statements about the decoupling behavior of the scalars  $\eta_i$ ,  $\eta_j$  and  $\eta_k$ . If the masses of  $\eta_i$  ( $\eta_k$ ) arise solely from the vev  $v_h$  ( $v_\phi$ ), then these scalars will exhibit non-decoupling from  $h$  ( $\phi$ ) as their masses are taken very large: if instead their masses include sources besides  $v_h$  or  $v_\phi$ , then decoupling will occur as the mass scale of these new sources is taken large. The behavior of the  $\eta_j$  states are a straightforward combination of the previous arguments.

For fermions, we write

$$\begin{aligned} \mathcal{M}(gg \xrightarrow[\text{fermions}]{} s_1) &= c_\theta \left[ \sum_i \mathcal{M}(gg \xrightarrow{\psi_i} h) + \sum_j \mathcal{M}(gg \xrightarrow{\psi_j} h) \right] \\ &- s_\theta \left[ \sum_j \mathcal{M}(gg \xrightarrow{\psi_j} \phi) + \sum_k \mathcal{M}(gg \xrightarrow{\psi_k} \phi) \right]. \end{aligned} \quad (12)$$

To be more illustrative, we can take some familiar examples to demonstrate the flexibility of Eq. (12). In the case with Higgs mixing but without new fermions  $\psi_j$  or  $\psi_k$ , then  $\psi_i$  consists of the SM quarks and we get a universal  $c_\theta$  suppression of the matrix element. If instead we only add a new vector-like top partner to the SM, then  $c_\theta = 1$ ,  $s_\theta = 0$ , and  $\psi_i$  includes the first five SM quarks and the two fermion mass eigenstates resulting from top mixing while the  $\psi_j$  and  $\psi_k$  sums are absent. Finally, if Higgs mixing is present and new colored fermions are added that couple both to  $h$  and  $\phi$  but do not mix with the SM fermions, then  $\psi_i$  will run over the SM quarks and  $\psi_j$  will run over the NP colored fermions.

Lastly, we can introduce massive colored vectors. We will only consider the case where these vectors couple to  $\phi$ , giving the relatively simple expression

$$\mathcal{M}(gg \xrightarrow[\text{vectors}]{} s_1) = -s_\theta \left[ \sum_k \mathcal{M}(gg \xrightarrow{V_k} \phi) \right], \quad (13)$$

emphasizing that this contribution to the gluon fusion rate for  $s_1$  production relies on the Higgs portal, since the SM Higgs is assumed to play no role in breaking the extended color gauge symmetry.

After the above discussion, we present a parametric understanding of how production and decays of  $s_{1,2}$  are affected by direct coupling and  $h$ - $\phi$  mixing. As we have seen, performing a completely

general analysis would be overly cumbersome, and so we will make a few mild assumptions to make the analysis more intuitive and tractable. Throughout the discussion, we assume a narrow width approximation, allowing us to factorize production and decay processes.

We define the overall leading order enhancement or suppression factor of  $s_1$  production relative to SM Higgs production via gluon fusion as

$$\epsilon_{gg} \equiv \frac{\sigma(gg \rightarrow s_1)}{\sigma(gg \xrightarrow{SM} h)} = \frac{|\mathcal{M}(gg \rightarrow s_1)|^2}{\left| \mathcal{M}(gg \xrightarrow{SM} h) \right|^2} = \frac{|c_\theta \mathcal{M}(gg \rightarrow h) - s_\theta \mathcal{M}(gg \rightarrow \phi)|^2}{\left| \mathcal{M}(gg \xrightarrow{SM} h) \right|^2} = c_\theta^2 |\mathcal{Z}_{ggh} - t_\theta \mathcal{Z}_{gg\phi}|^2, \quad (14)$$

using Eq. (9) and with  $t_\theta = \tan \theta$ . The complex amplitude ratios are given by

$$\mathcal{Z}_{ggh} \equiv \frac{\mathcal{M}(gg \rightarrow h)}{\mathcal{M}(gg \xrightarrow{SM} h)}, \quad \mathcal{Z}_{gg\phi} \equiv \frac{\mathcal{M}(gg \rightarrow \phi)}{\mathcal{M}(gg \xrightarrow{SM} h)}, \quad (15)$$

and will simplify significantly for any given NP model under consideration, as we will demonstrate in Secs. IV, V and VI. We see that both  $\epsilon_{gg} > 1$  (signaling enhancement) and  $\epsilon_{gg} < 1$  (signaling suppression) are possible with New Physics and changing the sign of  $\lambda_{hp}$ . In the limit that  $\theta = 0$ , the only effect on gluon fusion arises from the inclusion of new colored states that directly couple to the SM Higgs, which was a main focus of [19, 20, 32]. In the case where Higgs mixing is the only new effect, then  $\mathcal{Z}_{ggh} = 1$  and  $\mathcal{Z}_{gg\phi} = 0$ , and we have the simple expression  $\epsilon_{gg} = c_\theta^2$ , as noted in [27].

We remark that complete suppression of gluon fusion does not correspond to vanishing LHC production for the  $s_1$  state. This is because the subdominant modes of vector boson fusion, vector boson association, and  $t\bar{t}h$  production comprise 12.5% of the total cross section for a SM Higgs mass at 125 GeV [71]. Moreover, even if the leading order cancellation in Eq. (14) is exact, we expect NLO corrections, which can be as large as 20% in the case of colored stops [8], to make the cancellation imperfect.

### C. New Physics Effects on Decays of $s_{1,2}$

We now extend our discussion to include NP effects on decay widths for our scalar state  $s_1$ , which we take to be dominantly SM Higgs-like. We will not detail all of the (practically infinite!) possible final states for  $s_1$ , but will instead focus on the  $WW$ ,  $ZZ$ ,  $\gamma\gamma$ ,  $b\bar{b}$  and  $\tau^+\tau^-$  decay channels. For the  $WW$  final state, we write

$$\mathcal{M}(s_1 \rightarrow WW) = c_\theta \mathcal{M}(h \rightarrow WW) - s_\theta \mathcal{M}(\phi \rightarrow WW) \approx c_\theta \mathcal{M}(h \rightarrow WW), \quad (16)$$

and thus

$$\frac{\mathcal{B}(s_1 \rightarrow WW)}{\mathcal{B}(h \xrightarrow{SM} WW)} \approx c_\theta^2 \frac{\Gamma_h}{\Gamma_{s_1}} , \quad (17)$$

where we have assumed the tree-level coupling of  $hWW$  dominates the (typically loop-induced) coupling of  $\phi WW$ , and  $\Gamma_h$  and  $\Gamma_{s_1}$  are the total width of the purely SM Higgs and the mass eigenstate  $s_1$ , respectively. Under the same assumption that  $hZZ$  dominates the  $\phi ZZ$  coupling, the same result in Eq. (17) also applies to the  $ZZ$  final state, and so branching ratios of  $s_1$  to  $WW$  or  $ZZ$  diboson states are typically suppressed in Higgs mixing models.

For the diphoton final state, we can adapt our gluon fusion discussion, replacing colored particles with electromagnetically charged particles. Following the guide of Eq. (9), this gives

$$\mathcal{M}(s_1 \rightarrow \gamma\gamma) = c_\theta [\mathcal{M}(h \rightarrow \gamma\gamma)]|_{m_h=m_{s_1}} - s_\theta [\mathcal{M}(\phi \rightarrow \gamma\gamma)]|_{m_\phi=m_{s_1}} . \quad (18)$$

Unlike the  $WW$  or  $ZZ$  decay modes, the  $h \rightarrow \gamma\gamma$  decay is induced at loop level in the SM and new contributions can easily cancel against or add to the SM contributions. Using Eq. (18), we can write the relative branching ratio as,

$$\frac{\mathcal{B}(s_1 \rightarrow \gamma\gamma)}{\mathcal{B}(h \xrightarrow{SM} \gamma\gamma)} = \epsilon_{\gamma\gamma} \frac{\Gamma_h}{\Gamma_{s_1}} , \quad (19)$$

where  $\epsilon_{\gamma\gamma}$  is analogous to  $\epsilon_{gg}$  in Eq. (14) and  $\mathcal{Z}_{h\gamma\gamma}$  and  $\mathcal{Z}_{\phi\gamma\gamma}$  are defined similarly.

The relative rate for  $gg \rightarrow s_1 \rightarrow \gamma\gamma$  versus  $gg \rightarrow h \rightarrow \gamma\gamma$  is now given by

$$\mathcal{R} = \epsilon_{gg}\epsilon_{\gamma\gamma} \frac{\Gamma_h}{\Gamma_{s_1}} . \quad (20)$$

In many models, though, the various inputs for Eq. (20) reduce to simple expressions. For example, in Higgs mixing scenarios where  $\phi$  only couples to hidden sector particles, we obtain  $\mathcal{Z}_{h\gamma\gamma} = 1$ ,  $\mathcal{Z}_{\phi\gamma\gamma} = 0$ , and so

$$\frac{\mathcal{B}(s_1 \rightarrow \gamma\gamma)}{\mathcal{B}(h \xrightarrow{SM} \gamma\gamma)} = c_\theta^2 \frac{\Gamma_h}{\Gamma_{s_1}} , \quad (21)$$

which agrees with the universal  $c_\theta^2$  suppression noted in [27]. Another simple limiting case arises if we take  $\theta = 0$  and introduce new charged particles in the  $\gamma\gamma$  loop coupling to the Higgs. In this case,  $h \equiv s_1$  and we can write

$$\frac{\mathcal{B}(s_1 \rightarrow \gamma\gamma)}{\mathcal{B}(h \xrightarrow{SM} \gamma\gamma)} = \frac{\Gamma_h}{\Gamma_{s_1}} |\mathcal{Z}_{h\gamma\gamma}|^2 , \quad (22)$$

so that only the direct NP effects contribute.

Finally, we can calculate the  $s_1$  branching ratio to  $b\bar{b}$  or  $\tau^+\tau^-$ . If Higgs mixing is present, if  $\phi$  does not appreciably couple to the SM fermions, and if the SM fermions are not mixed with NP fermions, then the same results from Eq. (17) apply, substituting  $f\bar{f}$  for  $WW$ . A completely general expression, however, because of the possible presence of all of these effects, is unwieldy. As an explicit case, for the  $b\bar{b}$  final state, if we allow for  $h$ - $\phi$  mixing and introduce a coupling between  $\phi$  and  $b\bar{b}$ , we obtain

$$\frac{\mathcal{B}(s_1 \rightarrow b\bar{b})}{\mathcal{B}(h \xrightarrow{SM} b\bar{b})} = c_\theta^2 \frac{\Gamma_h}{\Gamma_{s_1}} |1 - t_\theta \mathcal{Z}_{\phi b\bar{b}}|^2, \quad (23)$$

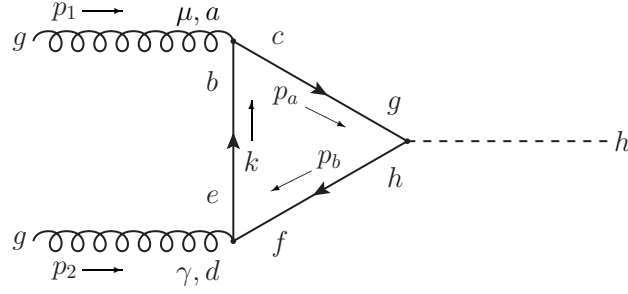
where  $\mathcal{Z}_{\phi b\bar{b}} = \mathcal{M}(\phi \rightarrow b\bar{b})/\mathcal{M}(h \xrightarrow{SM} b\bar{b})$ . We can see that interference effects from  $\mathcal{Z}_{\phi b\bar{b}}$ , although diluted by  $t_\theta$ , can lead to an overall increase in the branching fraction of  $s_1 \rightarrow b\bar{b}$ .

In summary, we have disentangled the effects from Higgs portal-induced mixing of  $h$  and  $\phi$  from NP effects caused by direct coupling to  $h$ ,  $\phi$ , or both. For gluon fusion, we have explicitly identified the decoupling behavior of New Physics states in Eqs. (11), (12) and (13). If we assume NP couplings to be small or negligible, then the resulting  $s_1$  branching ratio has a universal  $c_\theta^2$  suppression and a universal total width ratio suppression. On the other hand, interference effects resulting from couplings to  $h$  and/or  $\phi$  lead to a myriad of effects and possibilities for both suppression and enhancement of relative rates can be achieved.

We note that all of these expressions can readily be adapted for  $s_2$  decay with an appropriate  $c_\theta \rightarrow s_\theta$ ,  $-s_\theta \rightarrow c_\theta$  exchange and  $m_{s_1} \rightarrow m_{s_2}$ . In addition, if  $m_{s_2} > 2m_{s_1}$ , there is the additional decay mode  $s_2 \rightarrow s_1 s_1$ , as emphasized in [30]. Also, if any of the new states are lighter than  $m_{s_1}/2$  or  $m_{s_2}/2$ , then additional non-standard decay modes open up. This effect is manifest in the above expressions through the ratio of total widths  $\Gamma_h/\Gamma_{s_1}$ .

### III. THE $gg \rightarrow h$ PROCESS IN SM

Here we briefly review the leading order Standard Model calculation for Higgs production via gluon fusion. As shown in Fig. 1, gluon fusion arises in the SM via quark loops, with the dominant contribution coming from the top quark with its large Yukawa coupling. We again highlight the fact that since neither the  $W$  or  $Z$  boson couplings are probed in this production mode, large effects can be present in this loop process that strongly change Higgs production but do not affect EWSB.

FIG. 1. The Standard Model contribution to  $gg \rightarrow h$ .

The total Standard Model amplitude is

$$i\mathcal{M}_{SM}^{ad} = \sum_f i\mathcal{M}_f^{ad} = \sum_f i \left( \frac{\alpha_s}{\pi} \right) \frac{C(r_f)}{v_h} \delta^{ad} \epsilon_{1\mu} \epsilon_{2\nu} \left( p_1^\nu p_2^\mu - \frac{m_h^2}{2} g^{\mu\nu} \right) F_F(\tau_f) , \quad (24)$$

where  $f$  runs over the SM quarks,  $C(r_f)$  is the Casimir invariant ( $C(r_f) = 1/2$  for SM quarks),  $a$  and  $d$  are color indices,  $p_1 \cdot p_2 = \frac{m_h^2}{2}$  for an on-shell Higgs,  $\tau_f \equiv m_h^2/(4m_f^2)$  and  $F_F(\tau)$  is the well-known loop function

$$F_F(\tau) = \frac{2}{\tau^2} (\tau + (\tau - 1)Z(\tau)) , \quad (25)$$

using

$$Z(\tau) = \begin{cases} \arcsin^2 \sqrt{\tau} & \tau \leq 1 \\ \frac{-1}{4} \log \left[ \frac{1 + \sqrt{1 - \tau^{-1}}}{1 - \sqrt{1 - \tau^{-1}}} - i\pi \right]^2 & \tau > 1 . \end{cases} \quad (26)$$

Because the SM quarks obtain their mass purely from EWSB, they do not decouple even as we take the limit  $\tau \rightarrow 0$  (equivalent to  $m_f \rightarrow \infty$ ). In the case of the SM4, this sum would include  $t'$  and  $b'$  contributions. In the limit that the SM Higgs is well below the threshold for  $t$ ,  $t'$ , and  $b'$  to propagate on-shell in Fig. 1, we obtain the usual factor of 3 enhancement in the SM4 matrix element for  $gg \rightarrow h$ , which gives, at leading order, a factor of 9 enhancement for gluon fusion production in SM4 relative to SM3 [56]. Recent literature that has attempted to resolve the quandary of a sequential fourth generation of fermions with the lack of enhancement in gluon fusion include Refs. [52, 57–60].

We can anticipate, in the presence of new additions to gluon fusion coming from New Physics, that the main structure of Eq. (24) will not change apart from possible differences in the scalar vertex,  $C(r)$ , and the loop function  $F(\tau)$ . In particular, the  $p_1^\nu p_2^\mu - p_1 \cdot p_2 g^{\mu\nu}$  structure of the

matrix element is assured by  $SU(3)_c$  gauge invariance (or equivalently, the Ward identity). This is analogous to the situation in the  $h \rightarrow \gamma\gamma$  calculation, where electromagnetic gauge invariance requires the same momentum structure [68].

#### IV. NEW COLORED SCALAR

In this section, we isolate and calculate the effect of a colored complex scalar  $S$  propagating in the  $gg \rightarrow h$  loop. We use the Higgs portal in Eq. (2) to couple  $S$  to the SM Higgs, and we write a (positive) tree-level mass squared for  $S$  such that  $SU(3)_c$  remains unbroken and Higgs mixing is absent. Depending on the sign and strength of  $\lambda_{hp}$ , we can achieve significant suppression or enhancement of gluon fusion as a result of the interference between the SM fermions and the colored scalar.

The Lagrangian involving  $S$  is

$$\mathcal{L}_S = |D_\mu S|^2 - m_0^2 S^\dagger S - \kappa |S^\dagger S|^2 + \lambda_{hp} S^\dagger S H^\dagger H , \quad (27)$$

where color indices have been suppressed and we assume  $m_0^2 > 0$  and  $\kappa > 0$  to ensure stability. As discussed in Sec. II,  $\lambda_{hp}$  must be real: for positive (negative)  $\lambda_{hp}$ , we will get destructive (constructive) interference with the SM loop calculation, in agreement with [20, 35] (note we have a different sign convention for  $\lambda_{hp}$ ). After EWSB, the physical scalar mass is

$$m_S^2 \equiv m_0^2 - \lambda_{hp} v_h^2 , \quad (28)$$

which imposes the constraint that  $m_0^2 > \lambda_{hp} v_h^2$  to avoid portal symmetry breaking of  $SU(3)_c$ .

The two diagrams to calculate are shown in Fig. 2. Since  $S$  is complex, the matrix element for Fig. 2A needs to be multiplied by 2 to account for the charge conjugate diagram: if  $S$  were real, no factor of 2 is used and instead the matrix element for Fig. 2B must include a symmetry factor of (1/2).

The total amplitude corresponding to the diagrams in Fig. 2 for a complex scalar field propagating in the loop is

$$i\mathcal{M}_S^{ad} = i \left( \frac{\alpha_s}{\pi} \right) \left( \frac{C(r_S) \lambda_{hp} v_h}{4m_S^2} \right) \delta^{ad} \epsilon_{1\mu} \epsilon_{2\nu} (p_1^\nu p_2^\mu - \frac{m_h^2}{2} g^{\mu\nu}) F_S(\tau_S) , \quad (29)$$

where  $C(r_S)$  is the  $SU(3)_c$  Casimir invariant for  $S$ ,  $\tau_S = m_h^2/(4m_S^2)$  and the loop function  $F_S$  is defined to be

$$F_S(\tau) = \tau^{-1} - \tau^{-2} Z(\tau) , \quad (30)$$

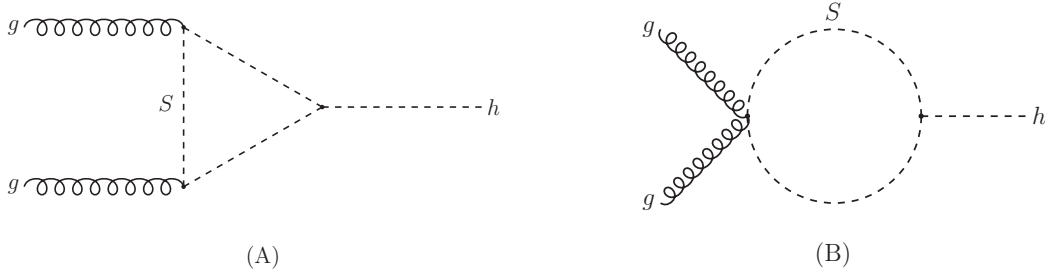


FIG. 2. Feynman diagrams for scalar loop contributions to  $gg \rightarrow h$ . For a complex scalar one must also include the charge conjugate equivalent of diagram (A).

with  $Z(\tau)$  defined in Eq. (26). Note that for fixed  $\lambda_{hp}$  the amplitude decouples as  $m_S \rightarrow \infty$  because of the tree-level mass squared  $m_0^2$ .

Now, the summed amplitude for  $\mathcal{M}(gg \xrightarrow{SM+S} h)$  is

$$\begin{aligned}
 i\mathcal{M}_{SM+S}^{ad} &= i \left( \sum_f \mathcal{M}_f^{ad} \right) + i\mathcal{M}_S^{ad} \\
 &= i \left( \frac{\alpha_s}{\pi} \right) \delta^{ad} \epsilon_{1\mu} \epsilon_{2\nu} (p_1^\nu p_2^\mu - \frac{m_h^2}{2} g^{\mu\nu}) \left( \sum_f \left( \frac{C(r_f)}{v_h} F_F(\tau_f) \right) + \frac{C(r_S) \lambda_{hp} v_h}{4m_S^2} F_S(\tau_S) \right).
 \end{aligned} \tag{31}$$

If  $m_S, m_t > m_h/2$ , then  $F_S$  is strictly real and negative and  $F_F$  is strictly real and positive, which implies that for  $\lambda_{hp} > 0$  ( $\lambda_{hp} < 0$ ) the interference between the colored scalar amplitude and the SM is destructive (constructive).

Since the phase space integration needed to calculate the  $s_1$  cross section is identical to the SM Higgs case, we can write the ratio  $\epsilon_{gg}$  from Eq. (14) as

$$\epsilon_{gg}|_{SM+S} = \frac{\left| \sum_f \left( \frac{C(r_f)}{v_h} F_F(\tau_f) \right) + \frac{C(r_S) \lambda_{hp} v_h}{4m_S^2} F_S(\tau_S) \right|^2}{\left| \sum_f \left( \frac{C(r_f)}{v_h} F_F(\tau_f) \right) \right|^2}. \tag{32}$$

We consider the addition of a real color octet scalar ( $C(r_s) = 3$ , symmetry factor of  $1/2$ ) and a complex color triplet scalar ( $C(r_s) = 1/2$ ) and plot  $\epsilon_{gg}$  in Fig. 3 as a function of  $m_S$  for some representative choices of parameters  $m_h$  and  $\lambda_{hp}$ . For the SM calculation, we sum over bottom and top quark contributions, using  $m_b = 4.20$  GeV and  $m_t = 172.5$  GeV. We adopt the results of [72] to draw vertical exclusion bands on light color octet scalars from ATLAS [73] and CMS [74] in dijet pair resonance searches. The gap in sensitivity from 200 GeV to 320 GeV between the  $34 \text{ pb}^{-1}$  ATLAS search and the  $2.2 \text{ fb}^{-1}$  CMS search is a result of the increased multijet trigger

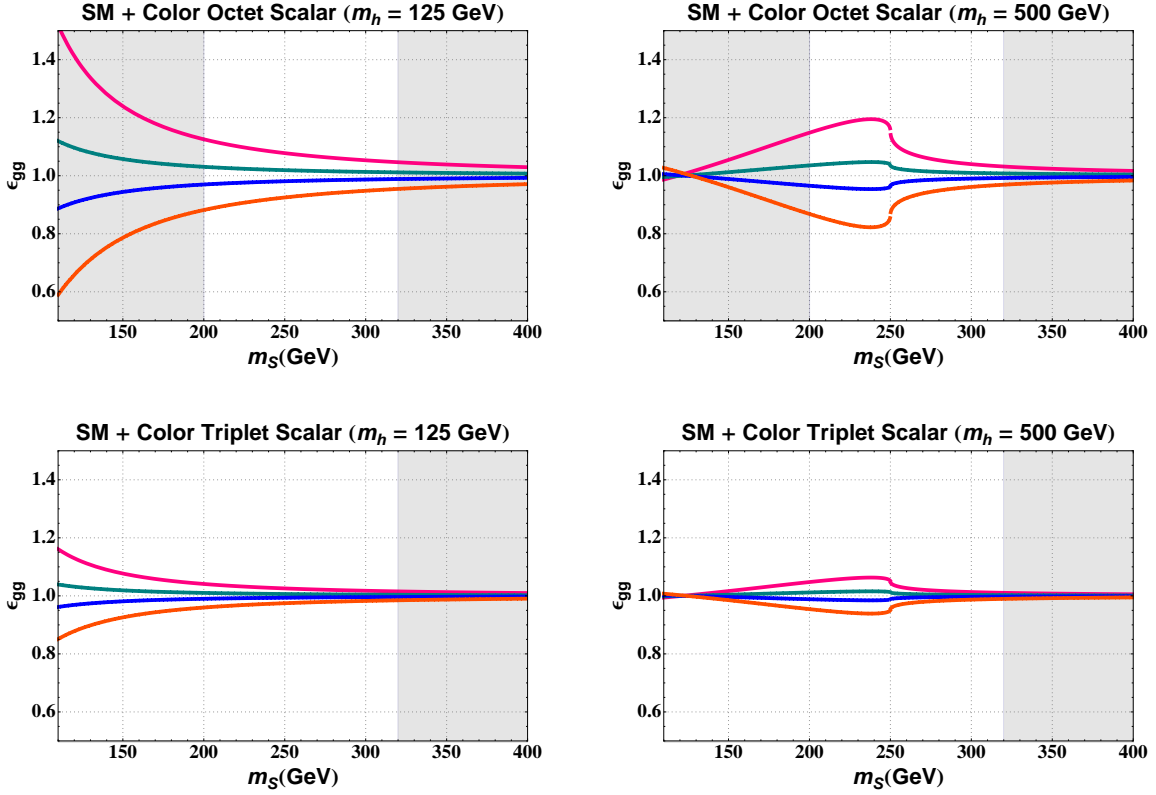


FIG. 3. Relative rate  $\epsilon_{gg}$  in Eq. (32), showing the effect of the inclusion of a real color octet scalar (top row) or complex color triplet scalar (bottom row), for  $m_h = 125$  GeV (left panels) or  $m_h = 500$  GeV (right panels). At the center of each plot, from top to bottom, the solid lines correspond to  $\lambda_{hp} = -0.2, -0.05, 0.05, 0.2$ . The left (right) gray bands in the octet scalar plots come from the ATLAS (CMS) search for pair produced dijet resonances. For the triplet case, the CMS bound still applies but the ATLAS bound is unconstraining after rescaling cross sections.

threshold to handle more difficult run conditions. In particular, for the CMS study, turn-on effects of the QCD multijet trigger made the background modeling unreliable below 320 GeV.

We see that both enhancement and suppression are possible, typically delineated by the choice of the sign of  $\lambda_{hp}$ . This is manifest in the region where  $m_S > m_h/2$  where  $\lambda_{hp} > 0$  corresponds to a suppression and  $\lambda_{hp} < 0$  corresponds to an enhancement. In the region where  $m_S < m_h/2$ , we see enhancement and suppression for both signs of  $\lambda_{hp}$  since the scalars can go on-shell in the loop, leading to an additional imaginary contribution to the scalar amplitude. The resulting interference is complicated by our inclusion of the bottom quark and its imaginary contribution, so the overall magnitude has competing cancellations among real and imaginary amplitude pieces. We note that Fig. 3 shows the expected decoupling of  $S$  as  $m_S$  grows. We also remark that for



negative values of  $\lambda_{hp}$ , our results are consistent with [20], where the finite difference in our results is a result of our inclusion of the bottom quark. Lastly, with regards to the ATLAS dijet pair search, we note that the complex triplet scalar is 1/9 the production cross section of the real octet scalar, if their masses are equal, rendering the search insensitive to complex triplet scalars.

## V. NEW COLORED FERMION

Adding new colored fermions to the Standard Model can greatly affect gluon fusion SM Higgs production in a number of unique ways. On one hand, new sequential generations of chiral fermions will add constructively with the SM fermion loops and, at leading order, scale the top quark loop by a multiplicative factor, as discussed in Sec. III. On the other hand, a new vector-like colored fermion that does not mix with SM fermions has no effect on gluon fusion. In general, a new colored fermion mass eigenstate comprised of chiral and vector-like components will enhance the SM Higgs gluon fusion rate according to the chiral projection of the mass eigenstate.

Because we also allow for Higgs portal-induced scalar mixing, though, the general situation can lead to either an overall suppression or enhancement of the gluon fusion rate. A model demonstrating the myriad of competing effects is straightforward to construct but only illuminating in its limiting cases. Hence, we will initially consider only mixing between a NP fermion and a SM fermion, neglecting the Higgs portal and Higgs mixing.

We add new vector-like top partners [75, 76], given by

$$\chi_{L,R} \sim (3, 1)_{2/3} . \quad (33)$$

This leads to the following mass terms,

$$\mathcal{L} \supset -y_t \tilde{H} \bar{Q}_L t_R - y_L \tilde{H} \bar{Q}_L \chi_R - M \bar{\chi}_L \chi_R + \text{h.c.} , \quad (34)$$

where  $M$  is a free parameter and  $y_L$  induces mixing between the SM top quark and  $\chi$ . In the  $(t, \chi)$  gauge basis, we have mass  $\hat{M}$  and interaction  $\hat{N}_h$  matrices given by

$$\hat{M} = \begin{pmatrix} M_t & \xi_L \\ 0 & M \end{pmatrix} , \quad \hat{N}_h = \begin{pmatrix} M_t & \xi_L \\ 0 & 0 \end{pmatrix} , \quad (35)$$

with  $\xi_L = \frac{y_L v_h}{\sqrt{2}}$  and  $M_t = \frac{y_t v_h}{\sqrt{2}}$ . Note the 0 entry in  $\hat{M}$  can always be ensured since it corresponds to the  $M' \bar{\chi}_L t_R$  operator, which can be trivially rotated away since  $\chi_R$  and  $t_R$  have the same quantum numbers. The mass basis rotation matrices are defined in the usual way from

$\hat{R}(\hat{M}^\dagger \hat{M})\hat{R}^\dagger = |\hat{M}_D|^2$  and  $\hat{L}(\hat{M}\hat{M}^\dagger)\hat{L}^\dagger = |\hat{M}_D|^2$ . After rotating  $\hat{M}$  and  $\hat{N}_h$  on the left (right) by a left-handed (right-handed) rotation matrix, we obtain

$$\mathcal{L} \supset -\bar{\mathbf{t}} \left( \hat{M}_D + \frac{h}{v_h} \hat{V}_h \right) P_R \mathbf{t} + \text{h.c.} , \quad (36)$$

where  $\mathbf{t} \equiv (t_1, t_2)$  and  $\hat{M}_D = \hat{L}\hat{M}\hat{R}^\dagger = \text{diag}(m_{t_1}, m_{t_2})$ ,  $\hat{V}_h = \hat{L}\hat{N}_h\hat{R}^\dagger$ . The coupling matrix  $\hat{V}_h$  dictates the couplings of the top sector to the SM Higgs and, in principle, can have off diagonal entries; however, only the diagonal entries contribute to  $gg \rightarrow h$ , because the  $\hat{L}$  and  $\hat{R}$  rotations leave the gauge interactions diagonal in the mass basis.

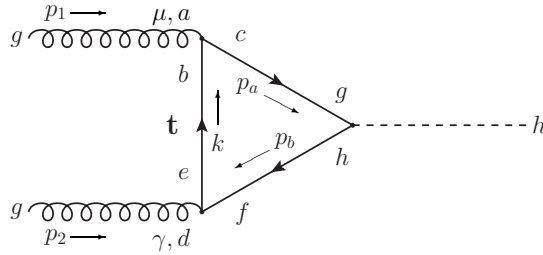


FIG. 4. Exotic fermion contribution in the mass eigenbasis.

In this top partner scenario, each mass eigenstate gives its own contribution to the diagrams in Fig. 4. Since  $SU(3)_c$  gauge invariance guarantees these two contributions differ only in their coupling to the Higgs via the element of  $\hat{V}_h$ , we can take the SM result for  $gg \rightarrow h$  through a top quark and insert the appropriate element of  $\hat{V}_h$  in place of the usual Yukawa coupling. This approach also encompasses more complicated mixing scenarios whereby the matrix element will exhibit different combinations of mixing angles and couplings for the various  $\hat{V}_h$  entries as a replacement for the  $hff$  vertex in the  $gg \rightarrow h$  amplitude. Since we are focused on exotic fermion effects on  $gg \rightarrow h$ , we take the  $(\hat{V}_h)_{ij}$  entry to be a free parameter, which can be readily calculated in any complete model.

The amplitudes involving exotic fermions in the loop are

$$i\mathcal{M}_F^{ad} = i \sum_i \left( \frac{\alpha_s}{\pi} \right) \left( \frac{(\hat{V}_h)_{ii}}{m_{F_i}} \right) \left( \frac{C(r_{F_i})}{v_h} \right) \delta^{ad} \epsilon_{1\mu} \epsilon_{2\nu} \left( p_1^\nu p_2^\mu - \frac{m_h^2}{2} g^{\mu\nu} \right) F_F(\tau_{F_i}) , \quad (37)$$

where the repeated indices on  $(\hat{V}_h)_{ii}$  are not summed,  $F_F(\tau)$  is given by Eq. (25),  $\tau_{F_i} \equiv m_h^2/(4m_{F_i}^2)$ , and  $F_i \in \{t_1, t_2\}$ . We see that the amplitude decouples as  $m_{F_i} \rightarrow \infty$ , unless  $m_{F_i}$  and  $(\hat{V}_h)_{ii}$  are generated by a common scale such as the Higgs vev. These direct new physics contributions

will alter  $gg \rightarrow h$  even in the absence of Higgs mixing. Generally these contributions will add constructively if  $(\hat{V}_h)_{ii} > 0$ .

Now, we augment the previous discussion to include Higgs mixing between  $h$  and a new scalar  $\phi$ . We replace the vector-like mass  $M$  in Eq. (34) by a Yukawa term which generates the desired mass term and a new interaction term involving  $\phi$  after  $\phi$  obtains a vev, giving

$$y_\phi \phi \bar{\chi}_L \chi_R \Rightarrow M(1 + \frac{\phi}{v_\phi}) \bar{\chi}_L \chi_R, \quad (38)$$

where  $M = \frac{y_\phi v_\phi}{\sqrt{2}}$ . We now have a second interaction matrix  $\hat{V}_\phi$ , which is added to Eq. (36) and defined analogously to  $\hat{V}_h$ , where

$$\hat{N}_\phi = \begin{pmatrix} 0 & 0 \\ 0 & M \end{pmatrix}. \quad (39)$$

As discussed in Subsec. II B, the  $t_1$ ,  $t_2$  loops will give an enhancement factor for gluon fusion production given by

$$\epsilon_{gg}|_{SM+\chi_{L,R}} = \frac{c_\theta^2 \left| \sum_{f, \text{ no } t} \left( \frac{C(r_f)}{v_h} F_F(\tau_f) \right) + \sum_i \left( \frac{C(r_{F_i})}{v_h} \left( \frac{(\hat{V}_h)_{ii}}{m_{F_i}} \right) F_F(\tau_{F_i}) - t_\theta \frac{C(r_{F_i})}{v_\phi} \left( \frac{(\hat{V}_\phi)_{ii}}{m_{F_i}} \right) F_F(\tau_{F_i}) \right) \right|^2}{\left| \sum_f \left( \frac{C(r_f)}{v_h} F_F(\tau_f) \right) \right|^2}. \quad (40)$$

Note that as  $m_{t_1, t_2} \rightarrow \infty$ ,  $t_1$  will decouple from the  $\phi$  component of  $s_1$  but not the  $h$  component, and vice versa for  $t_2$ .

We recognize that these new top partners will induce shifts in the electroweak oblique parameters  $S$  and  $T$ , but a full analysis of the allowed top partner parameter space is beyond the scope of this study. Therefore, we adapt the results from Ref. [19], which studied top partner effects on Higgs production and included the constraints from the  $S$  and  $T$  oblique corrections. We set  $m_\phi^2 > m_h^2$ , and for the vevs we are considering,  $-\lambda_{hp} v_h v_\phi$  is a small perturbation to the diagonal mass terms in Eq. (3), allowing us to approximate the  $s_1$  contribution to  $S$  and  $T$  by the Higgs contribution considered in [19] for equal masses. We can thus illustrate our main point, suppression of gluon fusion, in this phenomenologically viable top partner scenario. In Fig. 5 we plot contours of  $\epsilon_{gg}$  as a function of the left-handed fermion mixing angle and the heavy fermion mass eigenstate,  $m_{t_2}$  for representative values of  $\lambda_{hp}$ . The shaded bands correspond to regions consistent with the oblique parameters at the 68 % and 95 % C.L., taken from [19].

Separately, we can also consider new colored fermions which do not mix with the SM quarks. As a final example, we consider new electroweak singlet fermions  $\psi$  in the adjoint and fundamental representations of  $SU(3)_c$  which obtain mass from the new Yukawa term of Eq. (38) (with  $\chi \rightarrow \psi$ ). In particular, these fermions do not couple to  $h$ , and hence their effects will be suppressed by the scalar mixing angle in Eq. (5). The relative rate is now

$$\epsilon_{gg}|_{SM+\psi} = \frac{c_\theta^2 \left| \sum_f \left( \frac{C(r_f)}{v_h} F_F(\tau_f) \right) - t_\theta \left( \frac{C(r_\psi)}{v_\phi} F_F(\tau_\psi) \right) \right|^2}{\left| \sum_f \left( \frac{C(r_f)}{v_h} F_F(\tau_f) \right) \right|^2}. \quad (41)$$

We can see that  $\psi$  does not decouple from the  $gg \rightarrow s_1$  amplitude as its mass is taken very large because  $F_F(\tau_\psi)$  asymptotes to a finite value. We show  $\epsilon_{gg}$  in Fig. 6 for two choices of color representations. We see from Fig. 6 that the octet fermion (which includes a 1/2 to account for lack of conjugate diagram for a real fermion) produces larger suppression or enhancement than the triplet fermion for identical  $\lambda_{hp}$  values, as expected from the difference in their respective  $C(r_\psi)$ . Collider constraints on these new fermions will require model dependent assumptions about their decay channels, and since our focus is on the model independent effects on gluon fusion, we do not consider such constraints here.

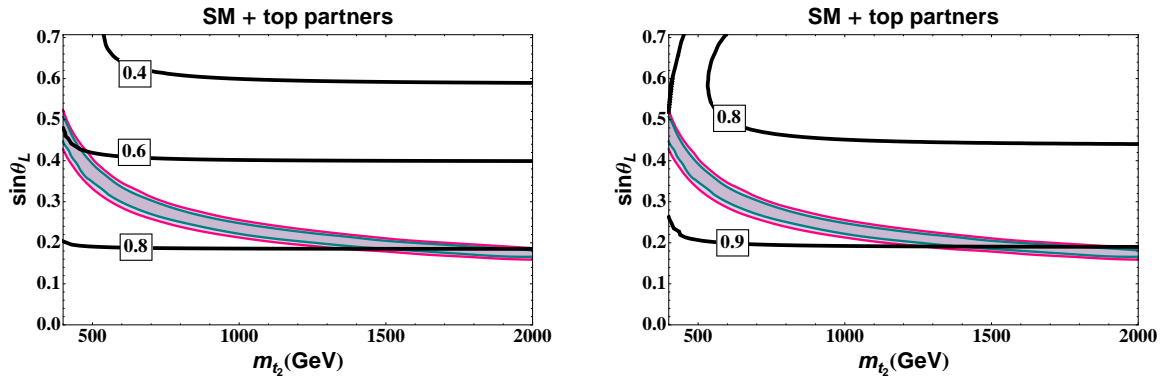


FIG. 5. Contours of the relative rate of  $s_1$  production as a function of  $m_{t_2}$  and the left-handed mixing angle in the top partner scenario for  $m_{s_1} = 800$  GeV,  $v_\phi = 500$  GeV, and  $\lambda_{hp} = -1$  (left) and 0.75 (right). We adapt the analysis and results of Ref. [19] to show shaded contours which are consistent with the oblique parameters  $S$  and  $T$  at the 68% and 95% C.L..

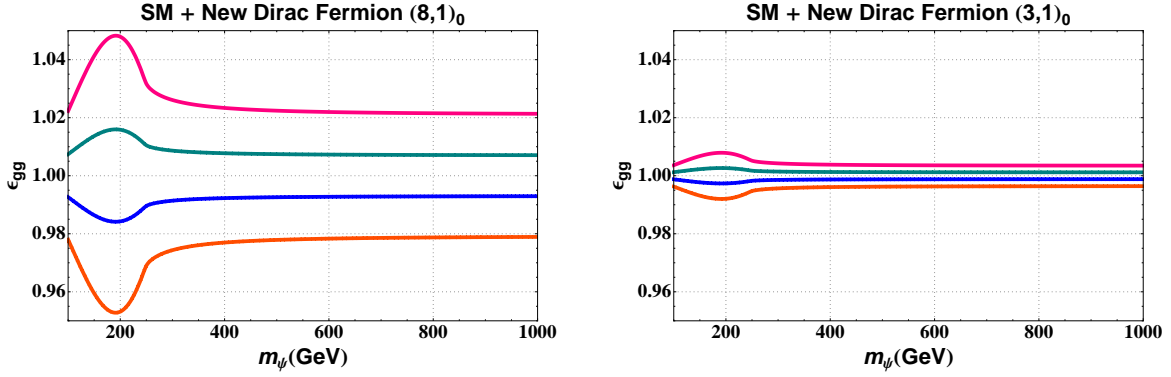


FIG. 6. Relative rate of  $s_1$  production with Higgs mixing and a new color octet fermion (left) and a new color triplet fermion (right). We choose  $v_\phi = 500$  GeV,  $m_{s_1} = 500$  GeV and  $m_{s_2} = 700$  GeV. From top to bottom, the solid lines in each plot correspond to  $\lambda_{hp} = 0.015, 0.005, -0.005, -0.015$ .

## VI. NEW COLORED VECTOR

The last type of New Physics contribution to gluon fusion we will consider is the addition of a new massive colored vector. In a renormalizable theory, the massive vector must arise from a spontaneously broken gauge theory, which necessarily entails the addition of a new scalar that acquires a vev and can mix with the SM Higgs via Eq. (2). Correspondingly, we will consider an extended gauge symmetry  $SU(3)_1 \times SU(3)_2$ , known as the renormalizable coloron model (ReCoM) [63, 64]. In this model, the complex scalar field  $\Phi$  transforms as  $(3, \bar{3})$  and obtains a diagonal vev (when written as a matrix-valued field), which breaks  $SU(3)_1 \times SU(3)_2$  to the diagonal subgroup, which is identified with the SM  $SU(3)_c$  symmetry. The  $\Phi$  field has 18 degrees of freedom: 8 are “eaten” by the broken gauge generators to make the massive color vector  $G'$  known as the coloron, 8 become a real scalar  $SU(3)_c$  octet  $G_H$ , and the remaining 2 are the real scalar  $\phi_R$  and pseudoscalar  $\phi_I$  color singlet fields. Hence, in this construction and a consequence of the Higgs portal, the addition of a massive color vector  $G'$  concomitantly includes a new scalar octet and two new scalar singlets, of which  $G_H$  necessarily affects gluon fusion and  $\phi_R$  mixes with the SM Higgs.

### A. The Renormalizable Coloron Model

We analyze the total scalar potential including the SM, the ReCoM, and the Higgs portal. Our analysis mirrors that found in [64], except our addition of the Higgs portal operator creates a link between the two scalar potentials  $V(H)$  and  $V(\Phi)$  and hence the two vevs must be solved for

simultaneously. The full scalar potential is

$$\begin{aligned}
V_{tot} &= V(\Phi) + V(H) + V_{hp} \\
&= -m_\Phi^2 \text{Tr}(\Phi^\dagger \Phi) - \mu_\Phi (\det \Phi + \text{h.c.}) + \frac{\lambda_\Phi}{2} [\text{Tr}(\Phi \Phi^\dagger)]^2 + \frac{\kappa_\Phi}{2} \text{Tr}(\Phi \Phi^\dagger \Phi \Phi^\dagger) \\
&\quad - m_H^2 |H|^2 + \lambda_H |H|^4 \\
&\quad - \lambda_{hp} |H|^2 \text{Tr}(\Phi^\dagger \Phi) ,
\end{aligned} \tag{42}$$

where we assume  $\mu_\Phi > 0$  without loss of generality. We require  $m_\Phi^2 > 0$  and  $m_H^2 > 0$  such that  $\Phi$  and  $H$  will acquire vevs. We also require  $3\lambda_\Phi + \kappa_\Phi > 0$  and  $\lambda_H > 0$  so each individual potential is bounded from below: we neglect renormalization group effects when discussing bounds on potential parameters.

It is straightforward to find the vevs for  $\Phi$  and  $H$  by decoupling the two equation system. We find, in analogy with [64],

$$\langle \Phi \rangle = \frac{v_\phi}{\sqrt{6}} \mathbb{I}_3 = \frac{\mu_\Phi + \sqrt{\mu_\Phi^2 + \left(2(3\lambda_\Phi + \kappa_\Phi) - \frac{3\lambda_{hp}^2}{\lambda_H}\right) \left(2m_\Phi^2 + \frac{\lambda_{hp} m_H^2}{\lambda_H}\right)}}{\left(2(3\lambda_\Phi + \kappa_\Phi) - \frac{3\lambda_{hp}^2}{\lambda_H}\right)} \mathbb{I}_3 . \tag{43}$$

If  $\lambda_{hp}$  is too large, then it can generate a new ground state at large field values of  $h$  and  $\phi$ . The resulting upper bound on  $\lambda_{hp}$  is  $\lambda_{hp}^2 < \frac{2}{3} \lambda_H (3\lambda_\Phi + \kappa_\Phi)$ , which we satisfy by requiring  $v_\phi > 0$ . Given Eq. (43), the Higgs vev is most easily written as

$$\langle H \rangle = \frac{1}{\sqrt{2}} \begin{pmatrix} 0 \\ v_h \end{pmatrix} = \frac{1}{\sqrt{2}} \begin{pmatrix} 0 \\ \sqrt{\frac{m_H^2}{\lambda_H} + \frac{\lambda_{hp} v_\phi^2}{2\lambda_H}} \end{pmatrix} , \tag{44}$$

and  $v_h$  is fixed to be 246 GeV.

Expanding  $\Phi$  around its vev, we get

$$\Phi = \frac{1}{\sqrt{6}} (v_\phi + \phi_R + i\phi_I) \mathbb{I}_3 + (G_H^a + iG_G^a) T^a , \tag{45}$$

where  $\phi_R$  and  $\phi_I$  are  $SU(3)_c$  singlets and  $G_H$  and  $G_G$  are  $SU(3)_c$  octets [64]. The  $G_G$  comprise the Goldstone bosons which give mass to the coloron,  $G'$ . The Higgs is decomposed in the usual way,

$$H = \frac{1}{\sqrt{2}} \begin{pmatrix} G^\pm \\ v_h + h + iG_o \end{pmatrix} \tag{46}$$

where  $G_o$  and  $G^\pm$  are the Goldstone bosons eaten by the electroweak gauge bosons.

After the spontaneous symmetry breaking  $SU(3)_1 \times SU(3)_2 \rightarrow SU(3)_c$  and EWSB, mixing is induced between the singlets  $\phi_R$  and  $h$ . This leads to the mass squared matrix in the  $(h, \phi_R)$  interaction basis given in Eq. (3) but with  $m_\phi^2 \rightarrow m_{\phi_R}^2$  and

$$m_h^2 = 2\lambda_H v_h^2, \quad m_{\phi_R}^2 = \frac{v_\phi^2}{3}(3\lambda_\Phi + \kappa_\Phi) - \frac{\mu_\Phi v_\phi}{\sqrt{6}}, \quad (47)$$

where  $v_h$  and  $v_\phi$  depend on  $\lambda_{hp}$ . The assumption of  $v_\phi > 0$  and the conditions  $0 \leq m_h^2 \leq m_{\phi_R}^2$  imply

$$\mu_\Phi < \sqrt{\frac{2}{3}}(3\lambda_\Phi + \kappa_\Phi)v_\phi. \quad (48)$$

By our assumptions, the right hand side of Eq. (48) is positive definite and thus bounds  $\mu_\Phi$  from above. Our analysis follows exactly the same steps as Subsec. II A, giving the following results:

$$\begin{aligned} \tan 2\theta &= \frac{-2\lambda_{hp}v_hv_\phi}{m_{\phi_R}^2 - m_h^2}, \\ s_1 &= h \cos \theta - \phi_R \sin \theta, \\ s_2 &= h \sin \theta + \phi_R \sin \theta. \end{aligned} \quad (49)$$

For the physical masses of  $s_1$  and  $s_2$ , we obtain

$$\begin{aligned} m_{s_1}^2 &= \frac{1}{2}(m_h^2 + m_{\phi_R}^2) - \frac{1}{2}\sqrt{(-m_h^2 + m_{\phi_R}^2)^2 + 4\lambda_{hp}^2 v_h^2 v_\phi^2}, \\ m_{s_2}^2 &= \frac{1}{2}(m_h^2 + m_{\phi_R}^2) + \frac{1}{2}\sqrt{(-m_h^2 + m_{\phi_R}^2)^2 + 4\lambda_{hp}^2 v_h^2 v_\phi^2}. \end{aligned} \quad (50)$$

For the physical masses of the remaining scalars in the spectrum we find,

$$m_{\phi_I}^2 = \sqrt{\frac{3}{2}}\mu_\Phi v_\phi, \quad m_{G_H}^2 = \frac{1}{3}(2m_{\phi_I}^2 + \kappa_\Phi v_\phi^2), \quad (51)$$

which agrees with [64] in the limit  $\lambda_{hp} \rightarrow 0$ .

The constraint  $m_{\phi_I}^2 > 0$  is satisfied since we assumed  $\mu_\Phi > 0$  and  $v_\phi > 0$ . Requiring  $m_{G_H}^2 > 0$  implies  $m_{\phi_I}^2 > -\kappa_\Phi v_\phi^2/2$ , which augments the previous condition Eq. (48) to give

$$-\frac{\kappa_\Phi v_\phi}{\sqrt{6}} < \mu_\Phi < \sqrt{\frac{2}{3}}(3\lambda_\Phi + \kappa_\Phi)v_\phi \quad (52)$$

In order for a valid range of  $\mu_\Phi$  to exist, we thus require

$$2\lambda_\Phi + \kappa_\Phi > 0. \quad (53)$$

Our subsequent analysis ensures these constraints are satisfied.

## B. Phenomenology

The diagrams for the colored vector loop in unitary gauge are shown in Fig. 7. Although the ReCoM model includes the  $G_H$  scalar octet contribution, we have isolated colored scalar amplitudes in Sec. IV, and so we focus here on the colored vector contribution.

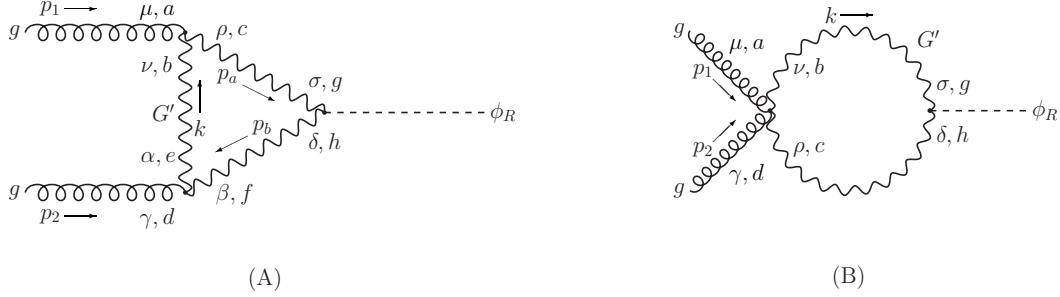


FIG. 7. Feynman diagrams for vector loop contributions to  $gg \rightarrow \phi_R$  in the unitary gauge.

The full amplitude for a real vector field propagating in the loop is

$$\begin{aligned} i\mathcal{M}_V^{ad} &= i\mathcal{M}_V^{ad}(gg \rightarrow \phi_R)|_{m_{\phi_R}=m_{s_1}} \\ &= i\left(\frac{\alpha_s}{\pi}\right)\left(\frac{C(r_{G'})}{4v_\phi}\right)\delta^{ad}\epsilon_{1\mu}\epsilon_{2\gamma}\left(p_1^\gamma p_2^\mu - \frac{m_{s_1}^2}{2}g^{\mu\gamma}\right)F_V(\tau_{G'}) \end{aligned} \quad (54)$$

where

$$F_V(\tau) \equiv -(\tau^{-1}(3+2\tau) + 3\tau^{-2}(-1+2\tau)Z(\tau)) \quad . \quad (55)$$

A full derivation of this amplitude in both unitary and Feynman gauge is presented in Appendix A.

The resulting enhancement factor is

$$\begin{aligned} \epsilon_{gg}|_{SM+ReCoM} &= \\ c_\theta^2 \frac{\left| \sum_f \left( \frac{C(r_f)}{v_h} F_F(\tau_f) \right) + \frac{1}{2} \frac{C(r_{G_H})}{4v_\phi} \left( \frac{\lambda_{hp} v_h v_\phi - t_\theta x_{G_H}}{m_{G_H}^2} \right) F_S(\tau_{G_H}) - t_\theta \left( \frac{C(r_{G'})}{4v_\phi} F_V(\tau_{G'}) \right) \right|^2}{\left| \sum_f \left( \frac{C(r_f)}{v_h} F_F(\tau_f) \right) \right|^2}, \end{aligned} \quad (56)$$

where  $x_{G_H}/v_\phi = (-m_{\phi_R}^2 + \frac{2}{3}m_{\phi_I}^2 - 2m_{G_H}^2)/v_\phi$  evaluated at  $m_{\phi_R} = m_{s_1}$  in Eq. (56) is the  $G_H$  coupling to  $\phi_R$  and we have included both  $G_H$  (with an explicit symmetry factor of 1/2) and  $G'$  contributions. We note that the real colored vector loop function  $F_{G'}$  is numerically about a factor of 5 larger and of the opposite sign than the usual SM loop function  $F_F$ . The scalar



loop function  $F_S(\tau)$  is also of the opposite sign and roughly a third of  $F_F$ : the loop functions are plotted in Fig. 8. We comment that, as a result of the large loop function for the colored vector, moderate values of  $\lambda_{hp}$  can have large effects on gluon fusion production. This provides a straightforward construction, for example, to counteract the enhancement from a fourth generation of chiral fermions in the Standard Model. If such a large cancellation of  $gg \rightarrow h$  amplitudes was present, however, we expect di-Higgs production via  $gg \rightarrow hh$  to be correspondingly enhanced if the  $gg \rightarrow hh$  triangle and bubble amplitudes are negligible: this is because the individual signs of direct Higgs couplings that lead to suppression become squared in the  $gg \rightarrow hh$  box amplitude. In this case, the di-Higgs gluon fusion production channel may be a promising discovery mode, and a more careful study is certainly warranted.

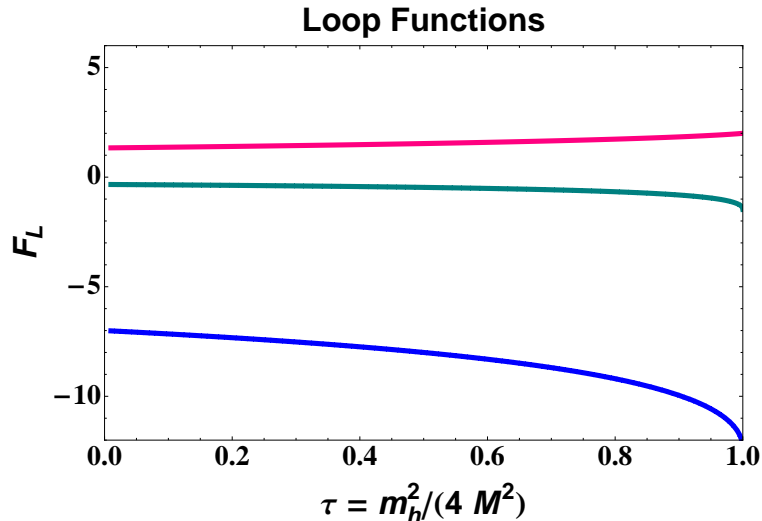


FIG. 8. Loop functions  $F_L = F_F$  (top),  $F_L = F_S$  (middle), and  $F_L = F_V$  (bottom) for fermion, scalar, and vector particles of mass  $M$ , respectively. The loop functions develop an imaginary part for  $\tau > 1$ , which corresponds to the particles in the loop going on-shell.

We first present results in Fig. 9 for  $\epsilon_{gg}$  with the sole addition of the colored vector for  $v_\phi = 200$  GeV and 3 TeV. The  $v_\phi = 200$  GeV choice is interesting because bounds on colorons in the low mass region coming from pairs of dijet resonances from ATLAS [73] and CMS [74] are not currently sensitive in the 200 to 320 GeV range, as discussed in Sec. IV. There are numerous recent studies which have done fits of the Higgs couplings to the data, including the Higgs-gluon effective coupling [77–80]. For  $v_\phi = 200$  GeV, a coloron mass of 250 GeV and mixing angle of  $s_\theta \sim -0.08$  one can reproduce the best fit point ( $c_g \sim 0.5$ ) for the scalar-gluon effective coupling found in [78]

and as can be seen from Fig. 9 one can also easily reproduce values which give rates close to the SM value should the effective coupling migrate towards the SM prediction with more data. We also consider  $v_\phi = 3$  TeV, which is the scale probed in dijet resonance searches using  $4 \text{ fb}^{-1}$  of 8 TeV LHC data at CMS [81]. The observed limit from this search on the coloron mass,  $m_{G'}$ , is 3.28 TeV. The bounds are indicated by gray vertical bands as described in the caption. The latest dijet resonance search done by the ATLAS collaboration [82] with  $5.8 \text{ fb}^{-1}$  of 8 TeV LHC data does not report an observed limit on the coloron mass but we expect the limit to be just a little higher because of the increased luminosity. An additional constraint on the coloron mass arises from the constraints imposed by ReCoM, whereby perturbativity restrictions on the original  $SU(3)_1 \times SU(3)_2$  gauge couplings give an upper limit and requirements on generating the correct  $SU(3)_c$  coupling give a lower limit. In deriving these bounds, which are given by dashed vertical lines in Fig. 9, we have neglected renormalization group running of  $\alpha_s$ .

In general, the ReCoM model includes contributions from the color vector  $G'$  and the scalar octet  $G_H$ . We can see from Eq. (56) that the contribution from  $G_H$  coming through the  $h$  component of  $s_1$  always adds constructively with the  $G'$  contribution. Whether the contribution from  $G_H$  entering through  $\phi_R$  also adds constructively with the  $G'$  contribution depends on the sign of  $x_{G_H}$ , which in turn depends on the mass hierarchy between the various scalars. We present the effect arising from only the color vector in the top row and from both new colored states in the bottom row of Fig. 9. For these plots, we have set  $m_{s_1} = 125$  GeV,  $m_{s_2} = 225$  GeV,  $m_{\phi_I} = 160$  GeV, and  $m_{G_H} = 140$  GeV.<sup>2</sup>

We remark that the flat behavior of  $\epsilon_{gg}$  in each plot arises because for  $m_{G'} > m_{s_1}$ , the loop function dependence of  $m_{G'}$  asymptotes quickly. This reflects the fact that as  $m_{G'}$  is taken large, its effects (which enter only through the  $\phi_R$  component of  $s_1$ ) do not decouple from the  $s_1$  production amplitude, which is reminiscent of the non-decoupling of  $W$  bosons from the SM Higgs in  $h \rightarrow \gamma\gamma$ . In addition, for the scalar octet  $G_H$ , which couples to both  $h$  and  $\phi_R$  components, we find that as  $m_{G_H}$  is taken large, its effects do not decouple from the  $\phi_R$  component but do decouple from  $h$ , see Sec. IV. Finally, we note the small reduction of  $\epsilon_{gg}$  in ReCoM is a result of the  $G_H$  contribution slightly cancelling the  $G'$  contribution, given our chosen parameter point for which  $x_{G_H} < 0$ , and we see that the overall effect is dominated by the coloron contribution, as expected from the magnitudes of the loop functions shown in Fig. 8.

---

<sup>2</sup> The ATLAS search for dijet pairs has an upward fluctuation above their expected limit in the 140 GeV range, which leaves the window of a scalar octet open for this mass point.

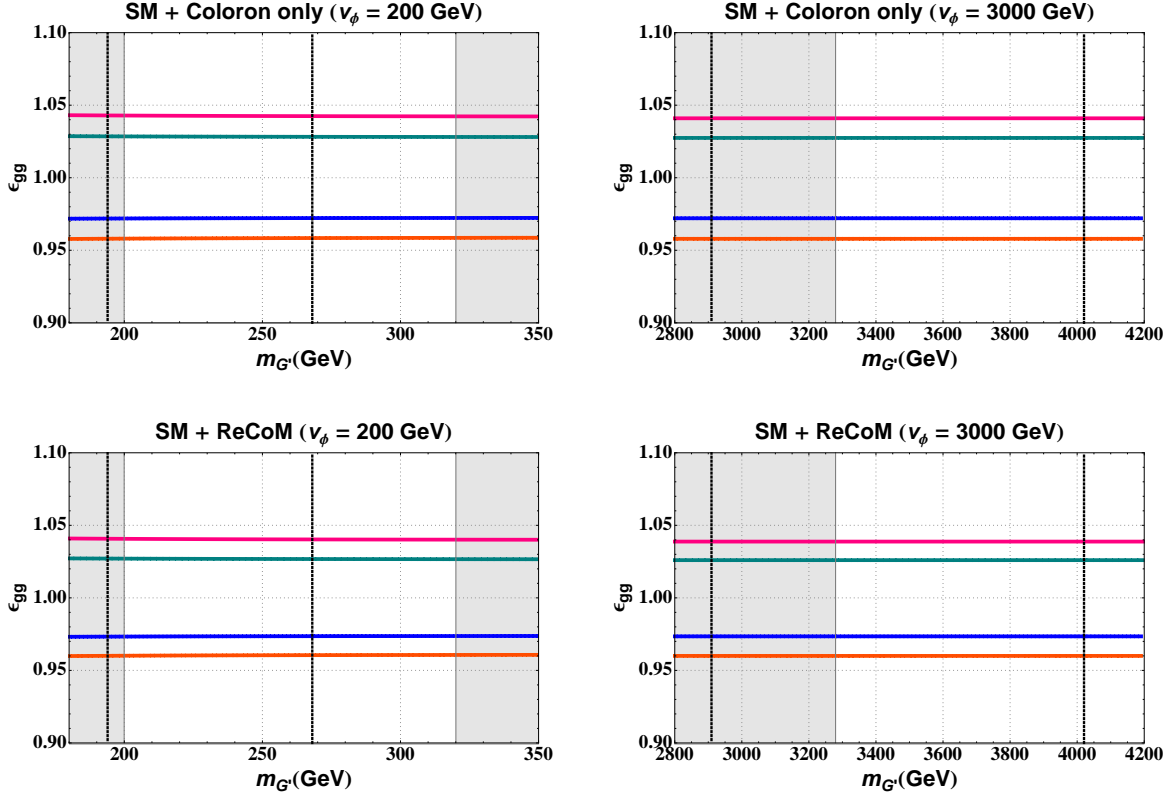


FIG. 9. Relative rate of  $s_1$  production showing the effect of adding only the coloron (top row) and the effect of adding the coloron and  $G_H$ , with  $m_{G_H} = 140$  GeV (bottom row). From top to bottom, the solid lines correspond to  $\lambda_{hp} = -0.0015, -0.001, 0.001, 0.0015$ . In the left panels, the gray bands correspond to the pair-produced dijet bounds from ATLAS (left) and CMS (right). In the right panels, the left gray band corresponds to the CMS exclusion on coloron production in dijet resonance searches. The left vertical dotted line corresponds to the minimum  $m_{G'}$  mass allowed given the specified choice of  $v_\phi$ , and the right vertical dotted line corresponds to the perturbativity constraint.

## VII. DISCUSSION AND CONCLUSION

We have seen that new colored particles can have significant effects on gluon fusion production. Also, the inclusion of Higgs portal-induced scalar mixing readily leads to new possibilities for suppressing or enhancing the gluon fusion rate. We have isolated contributions arising from new colored scalars, new colored fermions, including quark mixing, and new colored vectors. With the amplitudes in Eq. (29), Eq. (37), and Eq. (54), we can immediately calculate the interference effects present in general new physics models. We have demonstrated these effects can easily run from  $\mathcal{O}(1\%)$  to  $\mathcal{O}(10\%)$ , and both suppression and enhancement of gluon fusion can occur. Moreover, such large deviations are possible by colored states at mass scales that can be directly probed at

the LHC. In particular, when the effects on gluon fusion scale with the Higgs portal coupling  $\lambda_{hp}$ , the dearth of restrictions on  $\lambda_{hp}$  from the underlying theory can lead to very large modifications. If many competing effects are present in the  $gg \rightarrow h$  amplitude, we expect that di-Higgs production will be correspondingly altered and a promising discovery mode, but we leave a more careful study for future work.

Since gluon fusion production does not directly probe the Higgs mechanism or the phenomenon of electroweak symmetry breaking, Higgs identification studies should generally allow for mixing with a separate scalar state as well as competing effects from multiple new colored states running in the loop. Our general framework and analysis can be easily mapped onto the various recent studies which attempt to fit the data with non-SM Higgs couplings to two gluons. In particular we have shown that the various new physics effects can conspire to give rates very close to the SM expectation as well as easily accounting for any slight deviations as suggested by recent fits of the scalar effective couplings [77–80].

## ACKNOWLEDGEMENTS

The authors are grateful to Bill Bardeen, Marcela Carena, André de Gouvêa, Bogdan Dobrescu, Jennifer Kile, Ian Low, Adam Martin, Reinard Primulando, Pedro Schwaller, Daniel Stolarski, and Tim Tait for useful discussions. Fermilab is operated by Fermi Research Alliance, LLC under Contract No. De-AC02-07CH11359 with the United States Department of Energy.

## Appendix A: Vector Loop Calculation

In this appendix, we present the explicit calculation of the vector loop contribution to gluon fusion. As the loop calculation involves a particular choice of  $R_\xi$  gauge, we perform the calculation in both unitary ( $R_\xi \rightarrow \infty$ ) and Feynman ( $R_\xi = 1$ ) gauges. This calculation generalizes the well-known Standard Model calculation for  $h \rightarrow \gamma\gamma$  [45, 68, 83] to situations where a new “Higgs” field acquires a vev and leaves a non-Abelian gauge symmetry unbroken. In the SM, the Higgs field is responsible for spontaneously breaking  $SU(2)_L \times U(1)_Y$ , leaving the photon as the gauge field of the remaining Abelian  $U(1)_{em}$  gauge symmetry. In contrast, in the renormalizable coloron model (ReCoM),  $\Phi$  is responsible for spontaneously breaking  $SU(3)_1 \times SU(3)_2$ , leaving the gluon as the gauge field of the remaining non-Abelian  $SU(3)_c$  gauge symmetry. Then,  $gg \rightarrow \phi_R$  is the non-Abelian mirror version of  $h \rightarrow \gamma\gamma$ . We intuit that  $\mathcal{M}(gg \rightarrow \phi_R)$  is enhanced by a color factor

over the mirror process  $\mathcal{M}(h \rightarrow \gamma\gamma)$ , which is borne out from our calculation.

### 1. Vector Loop Amplitude: Unitary Gauge

We present the unitary gauge calculation of a colored vector contribution to gluon fusion. As mentioned above, we assume an extended color gauge symmetry that is partially broken by the vev of a new scalar field  $\Phi$ . After Higgs portal-induced mixing of  $h$  and  $\phi_R$ , the matrix elements  $\mathcal{M}(gg \rightarrow s_1)$  and  $\mathcal{M}(gg \rightarrow s_2)$  are simply related to  $\mathcal{M}(gg \rightarrow h)$  and  $\mathcal{M}(gg \rightarrow \phi_R)$  by

$$\begin{aligned}\mathcal{M}(gg \rightarrow s_1) &= c_\theta [\mathcal{M}(gg \rightarrow h)]|_{m_h=m_{s_1}} - s_\theta [\mathcal{M}(gg \rightarrow \phi_R)]|_{m_{\phi_R}=m_{s_1}} \\ \mathcal{M}(gg \rightarrow s_2) &= s_\theta [\mathcal{M}(gg \rightarrow h)]|_{m_h=m_{s_2}} + c_\theta [\mathcal{M}(gg \rightarrow \phi_R)]|_{m_{\phi_R}=m_{s_2}}.\end{aligned}\quad (\text{A1})$$

There are two diagrams which contribute to  $\mathcal{M}(gg \rightarrow \phi_R)$  in the unitary gauge, shown in Fig. 7 of the main text. The triangle diagram in Fig. 7A for the coloron insertion gives

$$\begin{aligned}i\mathcal{M}_A^{ad} &= -g_s^2 \left( \frac{2m_{G'}^2}{v_\phi} \right) f^{abc} f^{dcb} \epsilon_{1\mu} \epsilon_{2\gamma} \\ &\quad \int \frac{d^d k}{(2\pi)^d} \frac{V^{\mu\nu\rho} \left( g_{\alpha\nu} - \frac{k_\alpha k_\nu}{m_{G'}^2} \right) V^{\gamma\beta\alpha} \left( g_{\beta\delta} - \frac{p_{b\beta} p_{b\delta}}{m_{G'}^2} \right) g^{\sigma\delta} \left( g_{\sigma\rho} - \frac{p_{a\sigma} p_{a\rho}}{m_{G'}^2} \right)}{(k^2 - m_{G'}^2)(p_a^2 - m_{G'}^2)(p_b^2 - m_{G'}^2)},\end{aligned}\quad (\text{A2})$$

where  $p_a = k + p_1$ ,  $p_b = k - p_2$ , and the three-point vector vertex is

$$\begin{aligned}V^{\mu\nu\rho} &= (k + p_a)^\mu g^{\nu\rho} + (-p_a - p_1)^\nu g^{\rho\mu} + (p_1 - k)^\rho g^{\mu\nu} \\ V^{\gamma\beta\alpha} &= (p_b + k)^\gamma g^{\alpha\beta} + (p_2 - p_b)^\alpha g^{\gamma\beta} + (-k - p_2)^\beta g^{\alpha\gamma}.\end{aligned}\quad (\text{A3})$$

The amplitude for the bubble loop in Fig. 7B is

$$i\mathcal{M}_B^{ad} = -\left(\frac{1}{2}\right) g_s^2 \left( \frac{2m_{G'}^2}{v_\phi} \right) \epsilon_{1\mu} \epsilon_{2\gamma} \int \frac{d^d k}{(2\pi)^d} \frac{V_{acdb}^{\mu\rho\gamma\beta} g^{\sigma\delta} \left( g_{\delta\beta} - \frac{p_{a\delta} p_{a\beta}}{m_{G'}^2} \right) \left( g_{\rho\sigma} - \frac{k_\rho k_\sigma}{m_{G'}^2} \right)}{(p_a^2 - m_{G'}^2)(k^2 - m_{G'}^2)},\quad (\text{A4})$$

where  $p_a = p_1 + p_2 - k$ , a symmetry factor of  $\frac{1}{2}$  has been included, and the four-point vector vertex is

$$\begin{aligned}\delta^{bc} V_{acdb}^{\mu\rho\gamma\beta} &= -ig_s^2 \delta^{bc} (f^{ace} f^{dbe} (g^{\mu\gamma} g^{\rho\beta} - g^{\mu\beta} g^{\rho\gamma}) + f^{ade} f^{cbe} (g^{\mu\rho} g^{\gamma\beta} - g^{\mu\beta} g^{\gamma\rho}) \\ &\quad + f^{abe} f^{cde} (g^{\mu\rho} g^{\gamma\beta} - g^{\mu\gamma} g^{\rho\beta})) \\ &= -ig_s^2 f^{abe} f^{dbe} (2g^{\mu\gamma} g^{\rho\beta} - g^{\mu\beta} g^{\rho\gamma} - g^{\mu\rho} g^{\gamma\beta}).\end{aligned}\quad (\text{A5})$$

After expanding both Eqs. (A2) and (A4) using Feynman parameters, performing the loop momentum integration using Dimensional Regularization [84], and some simplification, we arrive at the summed amplitude

$$i\mathcal{M}_V^{ad} = i \left( \frac{\alpha_s}{\pi} \right) \left( \frac{C(r_{G'})}{4v_\phi} \right) \delta^{ad} \epsilon_{1\mu} \epsilon_{2\gamma} \left( p_1^\gamma p_2^\mu - \frac{m_{s_1}^2}{2} g^{\mu\gamma} \right) F_V(\tau_{G'}),\quad (\text{A6})$$

where  $C(r_{G'}) = 3$  for the coloron,  $\tau_{G'} = m_{s_1}^2/(4m_{G'}^2)$ , and the loop function  $F_V$  is given in the main text in Eq. (55). We remark that this result also agrees with the analogous SM calculation for  $h \xrightarrow{W} \gamma\gamma$  with the appropriate substitutions  $\alpha_s \rightarrow \alpha$ ,  $C(r) \rightarrow 1$ ,  $v_\phi \rightarrow v_h$ , and a factor of 2 included for the charge conjugate process [45, 68, 83].

## 2. Calculation: Feynman Gauge

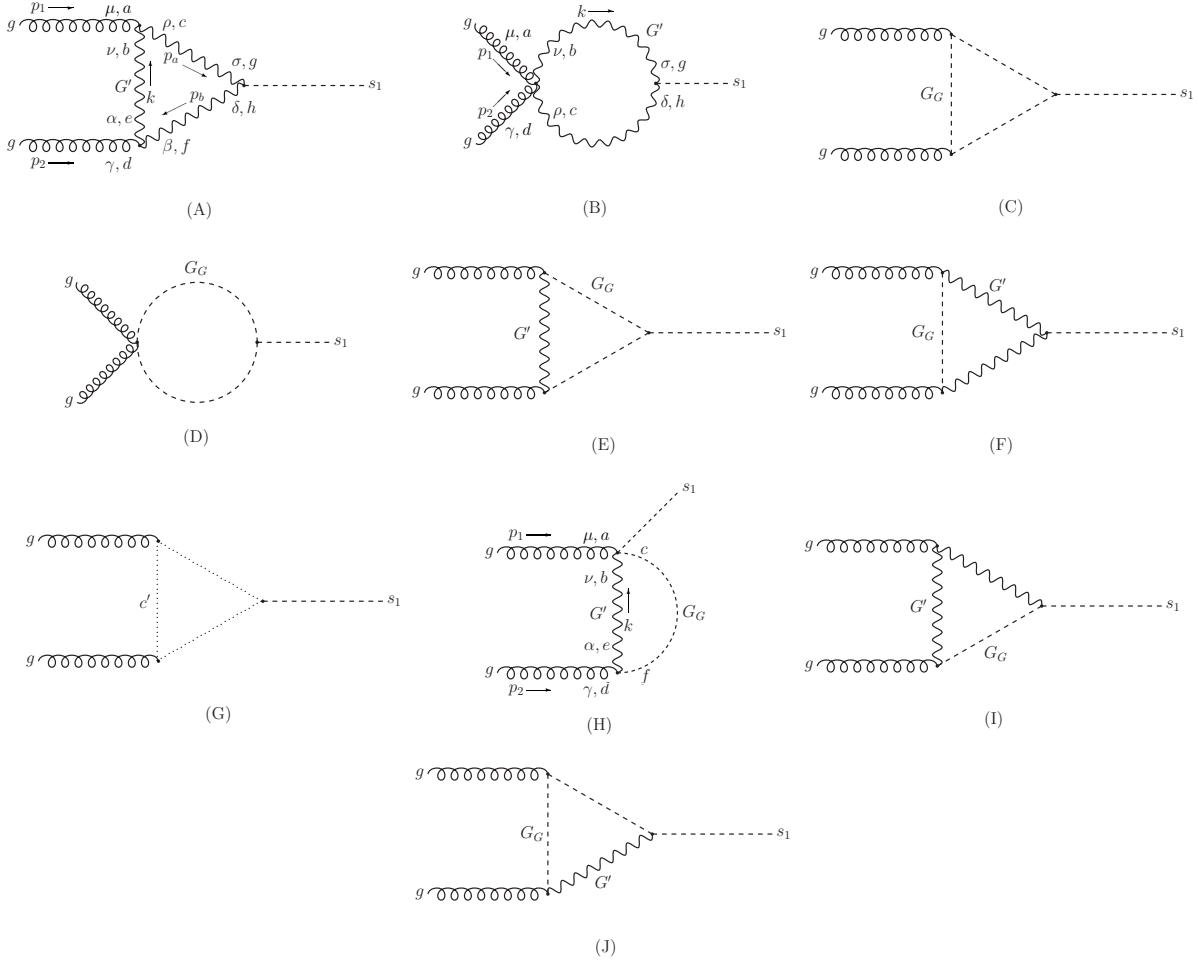


FIG. 10. Feynman diagrams for vector loop contributions to  $gg \rightarrow s_1$  in the Feynman gauge.

As a cross-check of our result in Subsec. A 1, we perform the same calculation in Feynman gauge, setting  $R_\xi = 1$ . Again, we adopt the ReCoM with the Higgs portal, as discussed in Subsec. VI A. In contrast to the calculation done in the unitary gauge, here we perform the calculation in the scalar mass basis, explicitly deriving the corresponding Goldstone couplings to  $s_1$  after taking into account the  $h$ - $\phi_R$  mixing. This motivates an interesting discussion of the coupling of Goldstone

bosons to their partner Higgs field when the partner Higgs field is mixed with spectator scalars and provides a further check that Higgs mixing and NP contributions to  $s_{1,2}$  production can be factored as in Eq. (A1).

### 3. Goldstone couplings

Beginning with the full scalar potential in Eq. (42) and the exact vacuum expectation values given in Eqs. (43) and (44), we examine the Goldstone couplings to the scalars  $h$  and  $\phi$ . After expanding the potential, we have

$$V(\Phi) \supset \frac{1}{2} G_G^a G_G^d \delta^{ad} \left( \phi_R \left( -\frac{\mu}{\sqrt{6}} + \frac{v_\phi}{3} (3\lambda_\Phi + \kappa_\Phi) \right) + h(-\lambda_H v_h) \right) + \frac{G_0^2}{2} (-\lambda_{hp} v_\phi \phi_R + 2\lambda_H v_h h) . \quad (\text{A7})$$

This can be written in matrix form as,

$$\begin{aligned} V(\Phi) &\supset \begin{pmatrix} h & \phi_R \\ \sqrt{2} & \sqrt{2} \end{pmatrix} \begin{pmatrix} 2\lambda_H v_h^2 & -\lambda_{hp} v_h v_\phi \\ -\lambda_{hp} v_h v_\phi & -\frac{\mu}{\sqrt{6}} v_\phi + \frac{v_\phi^2}{3} (3\lambda_\Phi + \kappa_\Phi) \end{pmatrix} \begin{pmatrix} \frac{G_0^2}{v_h \sqrt{2}} \\ \frac{G_G^a G_G^d \delta^{ad}}{v_\phi \sqrt{2}} \end{pmatrix} \\ &= \begin{pmatrix} h & \phi_R \\ \sqrt{2} & \sqrt{2} \end{pmatrix} \hat{M} \begin{pmatrix} \frac{G_0^2}{v_h \sqrt{2}} \\ \frac{G_G^a G_G^d \delta^{ad}}{v_\phi \sqrt{2}} \end{pmatrix} . \end{aligned} \quad (\text{A8})$$

Note if we set  $\lambda_{hp} = 0$ , then  $v_h$  and  $v_\phi$  become the unperturbed vevs and the Goldstone couplings become  $m_h^2/v_h$  and  $m_{\phi_R}^2/v_\phi$  for the original  $m_{\phi_R}^2$ ,  $m_h^2$ ,  $v_\phi$ , and  $v_h$ . From Eq. (A8) and Eq. (47) we see that the Goldstone–Goldstone–scalar interaction matrix  $\hat{M}$  is the same as the scalar mass matrix. Thus when we diagonalize the mass matrix, we will simultaneously diagonalize the Goldstone interaction matrix in Eq. (A8). Explicitly, we write the scalar mass and Goldstone interaction terms as

$$\mathcal{L} \supset - \begin{pmatrix} h & \phi_R \\ \sqrt{2} & \sqrt{2} \end{pmatrix} \hat{M} \begin{pmatrix} \frac{h}{\sqrt{2}} \\ \frac{\phi_R}{\sqrt{2}} \end{pmatrix} - \begin{pmatrix} h & \phi_R \\ \sqrt{2} & \sqrt{2} \end{pmatrix} \hat{M} \begin{pmatrix} \frac{G_0^2}{v_h \sqrt{2}} \\ \frac{G_G^a G_G^d \delta^{ad}}{v_\phi \sqrt{2}} \end{pmatrix} . \quad (\text{A9})$$

After diagonalization we obtain, for the interaction term,

$$\mathcal{L} \supset - \begin{pmatrix} s_1 & s_2 \\ \sqrt{2} & \sqrt{2} \end{pmatrix} \hat{M}_D \hat{U}^{-1} \begin{pmatrix} \frac{G_0^2}{v_h \sqrt{2}} \\ \frac{G_G^a G_G^d \delta^{ad}}{v_\phi \sqrt{2}} \end{pmatrix} \quad (\text{A10})$$

where  $\hat{M}_D = \hat{U}^{-1} \hat{M} \hat{U}$  is the diagonalized mass matrix with eigenvalues given in Eq. (50), and  $\hat{U}$  is the unitary rotation matrix with its mixing angle defined in Eq. (49). We see that the

Goldstone-Goldstone- $s_1$  interaction is

$$\mathcal{L} \supset -s_\theta \frac{m_{s_1}^2}{v_\phi} s_1 G_G^a G_G^d \delta^{ad}, \quad (\text{A11})$$

and so the Goldstone-Goldstone coupling to the scalar mass eigenstate is proportional to the scalar mass squared and a mixing angle. This justifies our ability to factor out the Higgs mixing angle when considering  $s_{1,2}$  production.

#### 4. Continuation of the Feynman Gauge Calculation

Returning to the calculation, there are ten diagrams in the Feynman gauge that must be calculated, as shown in Fig. 10. Using  $p_a = k + p_1$  and  $p_b = k - p_2$ ,  $p_c = p_1 + p_2 - k$ , Eq. (A3), and Eq. (A5), we obtain the amplitudes

$$i\mathcal{M}_A^{ad} = -2 \left( -s_\theta \frac{m_{G'}^2}{v_\phi} \right) g_s^2 f^{abc} f^{dcb} \epsilon_{1\mu} \epsilon_{2\gamma} \int \frac{d^d k}{(2\pi)^d} \frac{g_{\alpha\nu} g_{\beta\delta} g_{\sigma\rho} g^{\delta\sigma} V^{\mu\nu\rho} V^{\gamma\beta\alpha}}{(p_a^2 - m_{G'}^2)(p_b^2 - m_{G'}^2)(k^2 - m_{G'}^2)}, \quad (\text{A12})$$

$$i\mathcal{M}_B^{ad} = \left( \frac{1}{2} \right) \left( -s_\theta \frac{m_{G'}^2}{v_\phi} \right) \epsilon_{1\mu} \epsilon_{2\gamma} \int \frac{d^d k}{(2\pi)^d} \left( -ig_{\rho\beta} \delta^{bc} \right) V_{acdb}^{\mu\rho\gamma\beta} \frac{1}{(p_c^2 - m_{G'}^2)(k^2 - m_{G'}^2)}, \quad (\text{A13})$$

$$i\mathcal{M}_C^{ad} = -g_s^2 f^{abc} f^{dcb} \left( -s_\theta \frac{m_{s_1}^2}{v_\phi} \right) \epsilon_{1\mu} \epsilon_{2\gamma} \int \frac{d^d k}{(2\pi)^d} \frac{(p_a^\mu + k^\mu)(p_b^\gamma + k^\gamma)}{(p_a^2 - m_{G'}^2)(k^2 - m_{G'}^2)(p_b^2 - m_{G'}^2)}, \quad (\text{A14})$$

$$i\mathcal{M}_D^{ad} = -g_s^2 f^{bde} f^{bae} \left( -s_\theta \frac{m_{s_1}^2}{v_\phi} \right) \epsilon_{1\mu} \epsilon_{2\gamma} g^{\mu\gamma} \int \frac{d^d k}{(2\pi)^d} \frac{1}{(k^2 - m_{G'}^2)(p_c^2 - m_{G'}^2)}, \quad (\text{A15})$$

$$i\mathcal{M}_E^{ad} = g_s^2 m_{G'}^2 \left( -s_\theta \frac{m_{s_1}^2}{v_\phi} \right) f^{abc} f^{dcb} g^{\mu\gamma} \epsilon_\mu \epsilon_\gamma \int \frac{d^d k}{(2\pi)^d} \frac{1}{(k^2 - m_{G'}^2)(p_a^2 - m_{G'}^2)(p_b^2 - m_{G'}^2)}, \quad (\text{A16})$$

$$i\mathcal{M}_F^{ad} = 2g_s^2 m_{G'}^2 \left( -s_\theta \frac{m_{G'}^2}{v_\phi} \right) f^{abc} f^{dcb} g^{\mu\gamma} \epsilon_\mu \epsilon_\gamma \int \frac{d^d k}{(2\pi)^4} \frac{1}{(k^2 - m_{G'}^2)(p_a^2 - m_{G'}^2)(p_b^2 - m_{G'}^2)}, \quad (\text{A17})$$

$$i\mathcal{M}_G^{ad} = 2g_s^2 \left( -s_\theta \frac{m_{G'}^2}{v_\phi} \right) f^{abc} f^{dcb} \epsilon_{1\mu} \epsilon_{2\gamma} \int \frac{d^d k}{(2\pi)^d} \frac{k^\mu k^\gamma}{(p_a^2 - m_{G'}^2)(p_b^2 - m_{G'}^2)(k^2 - m_{G'}^2)}, \quad (\text{A18})$$

$$i\mathcal{M}_H^{ad} = 2g_s^2 f^{abc} f^{dcb} g^{\mu\gamma} \left( -s_\theta \frac{m_{G'}^2}{v_\phi} \right) \epsilon_{1\mu} \epsilon_{2\gamma} \int \frac{d^d k}{(2\pi)^d} \frac{1}{(k^2 - m_{G'}^2)(p_b^2 - m_{G'}^2)}, \quad (\text{A19})$$

$$i\mathcal{M}_I^{ad} = -2g_s^2 f^{abc} f^{dcb} \left( -s_\theta \frac{m_{G'}^2}{v_\phi} \right) \epsilon_{1\mu} \epsilon_{2\gamma} \int \frac{d^d k}{(2\pi)^d} \frac{g_{\alpha\nu} g_{\sigma\rho} g^{\alpha\gamma} V^{\mu\nu\rho} (k - p_1 - 2p_2)^\sigma}{(p_a^2 - m_{G'}^2)(p_b^2 - m_{G'}^2)(k^2 - m_{G'}^2)}, \quad (\text{A20})$$

$$i\mathcal{M}_J^{ad} = -2g_s^2 f^{abc} f^{dcb} \left( -s_\theta \frac{m_{G'}^2}{v_\phi} \right) \epsilon_{1\mu} \epsilon_{2\gamma} \int \frac{d^d k}{(2\pi)^d} \frac{g_{\beta\delta} g^{\beta\gamma} (k - p_2)^\delta (2k + p_1)^\mu}{(p_a^2 - m_{G'}^2)(p_b^2 - m_{G'}^2)(k^2 - m_{G'}^2)}. \quad (\text{A21})$$

After converting to Feynman parameters, calculating the loop integrals, summing all of the amplitudes, and some simplification, the divergences cancel and we obtain for the production of  $s_1$ ,

$$i\mathcal{M}_V^{ad} = -is_\theta \left( \frac{\alpha_s}{\pi} \right) \left( \frac{C(r_{G'})}{4v_\phi} \right) \delta^{ad} \epsilon_{1\mu} \epsilon_{2\gamma} \left( p_1^\gamma p_2^\mu - \frac{m_{s_1}^2}{2} g^{\mu\gamma} \right) F_V(\tau_{G'}), \quad (\text{A22})$$



in agreement with Eq. (A6) and Eq. (A1).

- 
- [1] G. Aad et al. (ATLAS Collaboration), Phys.Lett.B (2012), 1207.7214.
  - [2] S. Chatrchyan et al. (CMS Collaboration), Phys.Lett.B (2012), 1207.7235.
  - [3] 1094083 (2012), preliminary results prepared for the Winter 2012 Conferences, 1203.3774.
  - [4] M. Spira, A. Djouadi, D. Graudenz, and P. Zerwas, Nucl.Phys. **B453**, 17 (1995), hep-ph/9504378.
  - [5] T. Binoth and J. van der Bij, Z.Phys. **C75**, 17 (1997), hep-ph/9608245.
  - [6] J. L. Diaz-Cruz (2000), hep-ph/0008001.
  - [7] A. V. Manohar and M. B. Wise, Phys.Lett. **B636**, 107 (2006), hep-ph/0601212.
  - [8] M. Muhlleitner and M. Spira, Nucl.Phys. **B790**, 1 (2008), hep-ph/0612254.
  - [9] A. Djouadi and G. Moreau, Phys.Lett. **B660**, 67 (2008), 0707.3800.
  - [10] R. Bonciani, G. Degrossi, and A. Vicini, JHEP **0711**, 095 (2007), 0709.4227.
  - [11] C. Arnesen, I. Z. Rothstein, and J. Zupan, Phys.Rev.Lett. **103**, 151801 (2009), 0809.1429.
  - [12] I. Low, R. Rattazzi, and A. Vichi, JHEP **1004**, 126 (2010), 0907.5413.
  - [13] C. Bouchart and G. Moreau, Phys.Rev. **D80**, 095022 (2009), 0909.4812.
  - [14] R. Boughezal and F. Petriello, Nucl.Phys.Proc.Suppl. **205-206**, 289 (2010), 1006.5773.
  - [15] A. Azatov, M. Toharia, and L. Zhu, Phys.Rev. **D82**, 056004 (2010), 1006.5939.
  - [16] R. Boughezal, Phys.Rev. **D83**, 093003 (2011), 1101.3769.
  - [17] X. Ruan and Z. Zhang (2011), 1105.1634.
  - [18] C. Burgess, M. Trott, and S. Zuberi, JHEP **0909**, 082 (2009), 0907.2696.
  - [19] Y. Bai, J. Fan, and J. L. Hewett (2011), 1112.1964.
  - [20] B. A. Dobrescu, G. D. Kribs, and A. Martin (2011), 1112.2208.
  - [21] G. Belanger, A. Belyaev, M. Brown, M. Kakizaki, and A. Pukhov (2012), 1201.5582.
  - [22] V. Ilisie and A. Pich (2012), 1202.3420.
  - [23] M. Carena, S. Casagrande, F. Goertz, U. Haisch, and M. Neubert (2012), 1204.0008.
  - [24] A. Azatov, O. Bondu, A. Falkowski, M. Felcini, S. Gascon-Shotkin, et al. (2012), 14 pages, 8 figures, 1204.0455.
  - [25] A. Azatov and J. Galloway, Phys.Rev. **D85**, 055013 (2012), 31 pages, 8 figures, 1110.5646.
  - [26] J. Berger, J. Hubisz, and M. Perelstein (2012), 1205.0013.
  - [27] R. Schabinger and J. D. Wells, Phys.Rev. **D72**, 093007 (2005), hep-ph/0509209.
  - [28] R. Barbieri, T. Gregoire, and L. J. Hall (2005), hep-ph/0509242.
  - [29] B. Patt and F. Wilczek (2006), hep-ph/0605188.
  - [30] M. Bowen, Y. Cui, and J. D. Wells, JHEP **0703**, 036 (2007), hep-ph/0701035.
  - [31] C. Englert, T. Plehn, D. Zerwas, and P. M. Zerwas, Phys.Lett. **B703**, 298 (2011), 1106.3097.
  - [32] C. Cheung and Y. Nomura (2011), 1112.3043.

- [33] J. M. Arnold, M. Pospelov, M. Trott, and M. B. Wise, JHEP **1001**, 073 (2010), 0911.2225.
- [34] A. Djouadi, O. Lebedev, Y. Mambrini, and J. Quevillon, Phys.Lett. **B709**, 65 (2012), 1112.3299.
- [35] B. Batell, S. Gori, and L.-T. Wang (2011), 28 pages, 21 figures, 1112.5180.
- [36] L. Lopez-Honorez, T. Schwetz, and J. Zupan (2012), 14 pages, 3 figures, 1203.2064.
- [37] T. Cohen, D. E. Morrissey, and A. Pierce (2012), 1203.2924.
- [38] C. Englert (2012), 1204.4579.
- [39] A. Djouadi, A. Falkowski, Y. Mambrini, and J. Quevillon (2012), 1205.3169.
- [40] A. Y. Ignatiev and R. Volkas, Phys.Lett. **B487**, 294 (2000), hep-ph/0005238.
- [41] R. S. Gupta and J. D. Wells, Phys.Lett. **B710**, 154 (2012), 6 pages, 6 figures/ v2: all plots now made with the lighter Higgs mass equal to 125 GeV and other minor corrections made, to be published in Physics Letters B, 1110.0824.
- [42] M. Frank, B. Korutlu, and M. Toharia (2012), 1204.5944.
- [43] J. J. Heckman, P. Kumar, and B. Wecht (2012), 1204.3640.
- [44] H. de Sandes and R. Rosenfeld, Phys.Rev. **D85**, 053003 (2012), 1111.2006.
- [45] M. A. Shifman, A. Vainshtein, M. Voloshin, and V. I. Zakharov, Sov.J.Nucl.Phys. **30**, 711 (1979).
- [46] G. D. Kribs, T. Plehn, M. Spannowsky, and T. M. P. Tait, Phys.Rev. **D76**, 075016 (2007), 0706.3718.
- [47] M. Carena, S. Gori, N. R. Shah, and C. E. Wagner, JHEP **1203**, 014 (2012), 1112.3336.
- [48] N. D. Christensen, T. Han, and S. Su (2012), 34 pages, 41 figures, 1203.3207.
- [49] S. Casagrande, F. Goertz, U. Haisch, M. Neubert, and T. Pfoh, JHEP **1009**, 014 (2010), 1005.4315.
- [50] F. Goertz, U. Haisch, and M. Neubert, Phys.Lett. **B713**, 23 (2012), 1112.5099.
- [51] E. Arik, O. Cakir, S. A. Cetin, and S. Sultansoy, Phys.Rev. **D66**, 033003 (2002), hep-ph/0203257.
- [52] N. B. Schmidt, S. Cetin, S. Istin, and S. Sultansoy, Eur.Phys.J. **C66**, 1238 (2010), 0908.2653.
- [53] Q. Li, M. Spira, J. Gao, and C. S. Li, Phys.Rev. **D83**, 094018 (2011), 1011.4484.
- [54] C. Anastasiou, S. Buehler, E. Furlan, F. Herzog, and A. Lazopoulos, Phys.Lett. **B702**, 224 (2011), 1103.3645.
- [55] G. Passarino, C. Sturm, and S. Uccirati, Phys.Lett. **B706**, 195 (2011), 1108.2025.
- [56] A. Denner, S. Dittmaier, A. Muck, G. Passarino, M. Spira, et al. (2011), 1111.6395.
- [57] G. Guo, B. Ren, and X.-G. He (2011), 1112.3188.
- [58] X.-G. He and G. Valencia, Phys.Lett. **B707**, 381 (2012), 1108.0222.
- [59] A. Djouadi and A. Lenz (2012), 8 pages, 3 figures, 1204.1252.
- [60] E. Kuflik, Y. Nir, and T. Volansky (2012), 1204.1975.
- [61] K. Belotsky, D. Fargion, M. Khlopov, R. Konoplich, and K. Shibaev, Phys.Rev. **D68**, 054027 (2003), hep-ph/0210153.
- [62] E. H. Simmons, Phys.Rev. **D55**, 1678 (1997), hep-ph/9608269.
- [63] C. T. Hill and E. H. Simmons, Phys.Rept. **381**, 235 (2003), hep-ph/0203079.
- [64] Y. Bai and B. A. Dobrescu, JHEP **1107**, 100 (2011), 1012.5814.
- [65] T. Plehn and M. Rauch (2012), 1207.6108.

- [66] I. Low, J. Lykken, and G. Shaughnessy (2012), 1207.1093.
- [67] M. Shifman, A. Vainshtein, M. B. Voloshin, and V. Zakharov, Phys.Rev. **D85**, 013015 (2012), 7 pages, no figures/ the version accepted for publication in Physical Review, 1109.1785.
- [68] W. J. Marciano, C. Zhang, and S. Willenbrock, Phys.Rev. **D85**, 013002 (2012), 15 pages, 5 figures/ references added, 1109.5304.
- [69] J. M. Cornwall, D. N. Levin, and G. Tiktopoulos, Phys.Rev. **D10**, 1145 (1974).
- [70] K. Fujikawa, B. Lee, and A. Sanda, Phys.Rev. **D6**, 2923 (1972).
- [71] S. Dittmaier et al. (LHC Higgs Cross Section Working Group) (2011), long author list - awaiting processing, 1101.0593.
- [72] W. Altmannshofer, R. Primulando, C.-T. Yu, and F. Yu, JHEP **1204**, 049 (2012), 1202.2866.
- [73] G. Aad et al. (ATLAS Collaboration), Eur.Phys.J. **C71**, 1828 (2011), long author list - awaiting processing, 1110.2693.
- [74] CMS Collaboration, CMS-PAS-EXO-11-016 (2012).
- [75] D. Choudhury, T. M. P. Tait, and C. E. M. Wagner, Phys.Rev. **D65**, 053002 (2002), hep-ph/0109097.
- [76] K. Kumar, W. Shepherd, T. M. Tait, and R. Vega-Morales, JHEP **1008**, 052 (2010), 1004.4895.
- [77] D. Carmi, A. Falkowski, E. Kuflik, and T. Volansky, JHEP **1207**, 136 (2012), 1202.3144.
- [78] D. Carmi, A. Falkowski, E. Kuflik, and T. Volansky (2012), 1206.4201.
- [79] P. P. Giardino, K. Kannike, M. Raidal, and A. Strumia, JHEP **1206**, 117 (2012), 1203.4254.
- [80] G. Giudice, C. Grojean, A. Pomarol, and R. Rattazzi, JHEP **0706**, 045 (2007), hep-ph/0703164.
- [81] CMS Collaboration, CMS-PAS-EXO-12-016 (2012).
- [82] Tech. Rep. ATLAS-CONF-2012-088, CERN, Geneva (2012).
- [83] J. R. Ellis, M. K. Gaillard, and D. V. Nanopoulos, Nucl.Phys. **B106**, 292 (1976).
- [84] G. 't Hooft and M. Veltman, Nucl.Phys. **B44**, 189 (1972).